POLYHEDRAL BORANE ANIONS: INVESTIGATION

OF THE MECHANISM OF RETENTION

THESIS

Presented to the Graduate Council of
Texas State University-San Marcos
in Partial Fulfillment of
the Requirements

for the Degree

Master of SCIENCE

by

Barrett M. Matthews

San Marcos, Texas
December 2007

POLYHEDRAL BORANE ANIONS: INVESTIGATION

OF THE MECHANISM OF RETENTION

Committee Members Approved:

_____

Debra A. Feakes, Chair

_____

Rachell E. Booth

_____

Walter E. Rudzinski

Approved:

_____

J. Michael Willoughby
Dean of the Graduate College

ACKNOWLEDGEMENTS

I would first and foremost like to thank God and His son Jesus Christ for blessing me with Dr. Debra A. Feakes. Her knowledge, wisdom, insight, and patience have been invaluable to my research and career. Her devotion to my research and her availability was unfaltering, even when other matters arose; she was able to be there for me.

I would also like to thank members of the laboratory who assisted me: Jeff McVey, who laid the foundation for my research and was a reservoir of knowledge, and Jacqueline Smits, for her synthesis and analysis of the boron-containing compounds. In addition to my own laboratory colleagues, I would like to thank Devin Blass for his work with the native gels and Amy Perez for her expertise and knowledge of MALDI-TOF mass spectrometry.

This manuscript was submitted on August 13, 2007.

iv

TABLE OF CONTENTS

LIST OF TABLES

LIST OF FIGURES

Page

ix

LIST OF SCHEMES

Page

ABSTRACT

POLYHEDRAL BORANE ANIONS: INVESTIGATION

OF THE MECHANISM OF RETENTION

by

Barrett M. Matthews

Texas State University-San Marcos

December 2007

SUPERVISING PROFESSOR: DEBRA A. FEAKES

The current therapies for cancer, such as radiation, surgery, and chemotherapy, are lacking in specificity and incomplete removal of the cancer tissues. Radiation and chemotherapy both result in the damage or destruction of normal cells. The incomplete removal of the cells by surgery leaves more cells to regenerate and the cells could possibly migrate to other regions of the body. These flaws are exacerbated in aggressive forms of cancer such as *glioblastoma multiforme*. *Glioblastoma multiforme* occurs in the brain, which profoundly affects the severity of destruction and or damage to the cells around the tumor. The ineffectiveness of these treatments, both adjunctively and synergistically, has lead to a need for a different method of treatment.

Boron neutron capture therapy (BNCT) is a binary cancer therapy believed to be an improved method to treat aggressive forms of cancer. The first step of the therapy

requires the localization of the boron-10 isotope in the tumor cells. Once the boron-10 isotope is localized, the area is irradiated by neutrons, ultimately resulting in the formation of an α-particle, a lithium particle, and a large amount of energy. The linear energy transfer from the fission process dissipates within the distance of one cell diameter and causes death of the cell where the boron-10 isotope was located. The development of BNCT has been limited by the lack of boron-containing compounds that are taken up and retained in the tumor cells.

One method that has been utilized to deliver boron-containing compounds specifically to the interior of the tumor cells is incorporation of the compounds into unilamellar liposomes. A variety of polyhedral borane anions have been encapsulated into unilamellar liposomes and evaluated in murine biodistribution experiments. Based on the results of the experiments, three mechanisms of retention have been proposed. The first mechanism is nucleophilic attack at the electron-deficient binding region of, for example, the $[n\text{-}B_{20}H_{18}]^{2-}$ ion. The second mechanism of retention is oxidation of the reduced anions, such as the $[ae\text{-}B_{20}H_{17}NH_3]^{3-}$ ion, to the oxidized species, such as the $[n\text{-}B_{20}H_{17}NH_3]^{-}$ ion, which is susceptible again to nucleophilic attack. The third mechanism involves thiol-containing ions, such as the $[a^2\text{-}B_{20}H_{17}SH]^{4-}$ ion, and is based on the proposed formation of a disulfide bond between the polyhedral borane anion and an intracellular protein sulfhydryl moiety on a cysteine residue.

The evaluation of the products formed from the reaction of three polyhedral borane anions, $[a^2\text{-}B_{20}H_{17}SH]^{-4}$, $[n\text{-}B_{20}H_{18}]^{2-}$, and $[ae\text{-}B_{20}H_{17}OH]^{4-}$, with select biomolecules was the focus of this research. The products of the reactions were evaluated using ^1H and ^{13}C NMR spectroscopy, COSY and HETCOR NMR experiments,

electrospray ionization (ESI) mass spectrometry, matrix assisted laser desorption

ionization time of flight (MALDI-TOF) mass spectrometry, sodium dodecyl sulfate

polyacrylamide gel electrophoresis (SDS-PAGE), and native PAGE. The ^{13}C NMR

spectrum of the product of the reaction between cysteine and the $[a^2\text{-}B_{20}H_{17}SH]^{-4}$ ion and

the product of the reaction between reduced glutathione and the $[a^2\text{-}B_{20}H_{17}SH]^{-4}$ ion both

exhibited a shift in the peak assigned to the β-carbon of cysteine. The ESI-MS spectrum

of the product formed from the reaction between reduced glutathione and the $[a^2\text{-}$

$B_{20}H_{17}SH]^{-4}$ ion contained a new product peak which was attributed to the formation of a

covalent bond between the two molecules. The SDS-PAGE and the native PAGE were

used to evaluate the reaction of human serum albumin (HSA) with the polyhedral borane

ions. The SDS-PAGE results were uninformative due to the association of the HSA with

itself under the reaction conditions; however, the native PAGE yielded a difference in

migration of the product formed from the reaction between HSA and the $[a^2\text{-}B_{20}H_{17}SH]^{-4}$

ion and the control HSA which was consistent with a strong interaction between the two

molecules. The results from the MALDI-TOF experiment contained too much of the

keratin contaminant and lacked the peaks characteristic of even the control HSA

spectrum. The combination of the experiments provide significant evidence of the ability

of the $[a^2\text{-}B_{20}H_{17}SH]^{4-}$ ion to form a covalent disulfide bond with biomolecules that

contain a cysteine amino acid. The $[n\text{-}B_{20}H_{18}]^{2-}$ and $[ae\text{-}B_{20}H_{17}OH]^{4-}$ ions did not exhibit

any results with cysteine, reduced glutathione, or HSA, which would be consistent with

the formation of a covalent bond.

1.0 INTRODUCTION

Current therapies for cancer lack specificity for the tumor cells, increasing damage to patients, and resulting in the incomplete removal of the tumor. Therapies such as radiation, surgery, and chemotherapy fall into this category. Radiation kills tumor cells due to an increased sensitivity of the tumor cells compared to the normal cells.[1] The amount of radiation used to ensure complete elimination of the tumor cells will also damage surrounding normal cells.[1] Chemotherapy treatments attack all rapidly dividing cells. As a result, white blood cells are also destroyed, which weakens the immune system of the patient. Surgery can be used to remove the tumors, but often remnant cells are left that can result in regeneration of the tumor in the same or different locations.[1]

The flaws in current therapies are exacerbated in aggressive forms of cancer such as *glioblastoma multiforme*. *Glioblastoma multiforme* occurs in the brain, profoundly increasing the severity of the damage, and the consequences resulting from the cancer therapies. Surgical removal of the tumors does not typically lead to relocation of the tumor, but the tumor often does show recurrence.[2] Highly malignant tumors display increased resistance to both radiation and chemotherapy, while the damage to the normal brain cells is severe.[3-4] Traditional therapies have been used, both adjunctively and synergistically, with little improvement in results. Poor results of the current therapies lead to a need for a more specific method of eradication of cancer, especially in the brain.

Boron neutron capture therapy (BNCT) is a binary therapy believed to be an improved method to treat aggressive forms of cancer, such as *glioblastoma multiforme*. Primarily developed for brain tumors, the therapy has also been used for metastatic melanoma and can, in theory, be used for all cancers. BNCT is unique in that, ideally, a minimum number of normal cells are affected by the treatment and only a single, relatively low irradiation intensity, is required.

The two step process begins with the localization of the boron-10 isotope in the interior of the tumor cells. Once the compound is localized, thermal neutron irradiation is applied to the tumor, resulting in the formation of a highly energetic boron-11 isotope.[5] The isotope divides into one lithium and one alpha (α) particle. The fission that occurs creates energy that is distributed is a distance of approximately one cell diameter (10 μm), and thus, causes death to the tumor cells that contained the boron-10 atoms.[5] For this therapy to be successful, the boron must be retained in the cell at a concentration of >15 µg of boron per g of tumor.[6] Calculations have estimated that the ratio of the concentration of the boron in the tumor to the concentration of boron in the normal tissue needs to be approximately 5:1, while the ratio of the concentration of boron in the tumor to the concentration of boron in the blood needs to be approximately 3:1.[1] Therefore, the boron compound must be highly specific and must be retained in the tumor.

The majority of the compounds that have been investigated to date have been administered as free compounds or as polyhedral borane anions encapsulated in unilamellar lipsosomes. The free compounds, such as borocaptate sodium (BSH, **Figure 1**),[1] *p*-boronophenylalanine (*p*-BPA, **Figure 2**),[1] nucleosides,[7] nucleotides,[7] and immunoconjugates[8] are taken up and retained based on structure or properties.
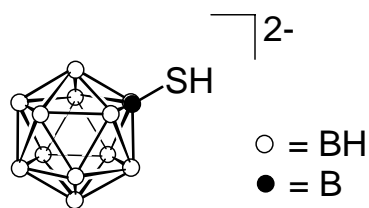
Figure 1: Structure of the $[B_{12}H_{11}SH]^{2-}$ anion (BSH).
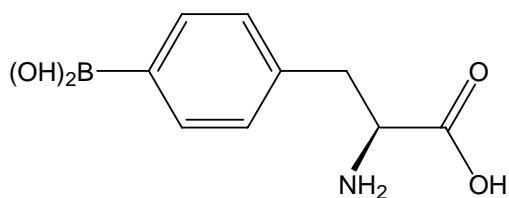
Figure 2: Structure of *p*-BPA.

The retention of BSH in the tumor cells is a result of the free sulfhydryl substituent.[9] Originally, researchers believed that the BSH was bound within the tumor cell as a result of disulfide bond formation with the thiol groups on the intracellular proteins in the tumor; however, no evidence exists to support this hypothesis.[9] *p*-BPA is thought to be taken up by rapidly growing tumor cells because of the constituent amino acid phenylalanine attached to the boron and the potential of the modified amino acid to be taken up in normal metabolic pathways.[10-12] Nucleosides are believed to be selective because of the high mitotic rates of tumor cells and retained by conversion to nucleosides or inclusion into tumor cell DNA.[7] Tumor specific immunoproteins are thought to adhere specifically to tumor cells and, with the synthesis of immunoconjugates, able, at least in concept, to deliver adequate amounts of boron to the tumor.[8] Most recently, tumor specific unilamellar liposomes have been used to deliver polyhedral borane anions having

no inherent tumor specificity.[9,13-15] The encapsulated polyhedral borane anions are delivered to the tumor mass based on the tumor selectivity of the liposomes and the boron is retained, in theory, by the potential reactivity of the specific anions.[9,13-15]

The specificity of the liposomes results from their small size (50-80 nm) and their ability to seep through the porous vasculature of rapidly growing tumor cells.[9,13-15] The uptake of the liposomes into the interior of the tumor cells is hypothesized to be a coated pit-coated vesicle mechanism into the cell.[16] The coated pit allows acidification of the liposome, which allows the release of the compound inside the liposome into the cytoplasm.[16]

The liposomal formulations were evaluated through the use of murine biodistribution studies.[9] The biodistribution experiments were performed using female BALB/c mice with EMT6 mammary adenocarcinoma, a mouse breast tumor, implanted into the right flank of the mouse 7-10 days before the experiment. The liposome emulsion was injected into the tail vein and the mice were sacrificed at five time points. At each time point, the blood, tumor, liver, and spleen were removed and sent for bulk boron analysis using inductively coupled plasma atomic emission spectroscopy (ICP-AES). An average of five mice per time point were used to collect the data. The retention of the boron was evaluated by measuring the concentration of boron in the tumor at each time point in μg of boron/g of tumor, while the specificity of the boron for the tumor was evaluated by measuring the tumor to blood ratio. The studies showed that water-soluble polyhedral borane anions could be delivered to the tumor cells inside unilamellar liposomes and that specific compounds could be retained in therapeutic amounts.[9]

However, the mechanism of the retention of the boron-containing compounds remains unknown.

The compounds used in the liposomes were, primarily, derivatives of the [n-B$_{20}$H$_{18}$]$^{2-}$ and [B$_{20}$H$_{18}$]$^{4-}$ anions. The two parent polyhedral borane anions, [n-B$_{20}$H$_{18}$]$^{2-}$ and [B$_{20}$H$_{18}$]$^{4-}$, have unique reactivity and can be substituted with appropriate reactive groups to enhance the retention of the boron-containing compounds in the tumor. The water-soluble polyhedral borane anions are believed to be retained by one of three mechanisms: nucleophilic attack, oxidation, or the formation of disulfide bonds. Any anion lacking appropriate reactivity is cleared from all tissues, including the tumor.

The first proposed mechanism is based on the nucleophilic attack of the electron-deficient bonding region characteristic of the [n-B$_{20}$H$_{18}$]$^{2-}$ anion and its derivatives (**Scheme I**).[9]
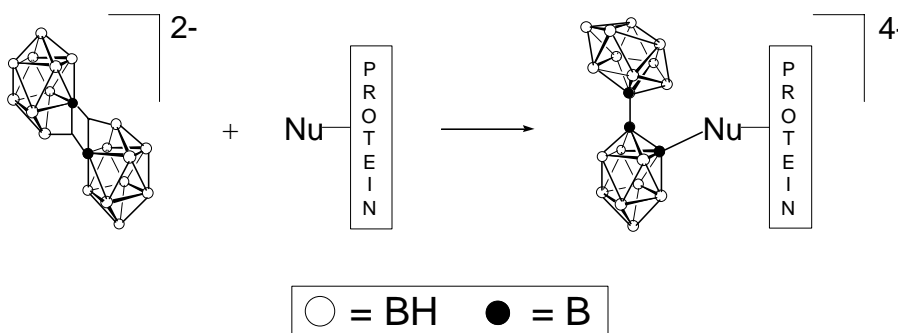
Scheme I: Proposed mechanism of retention by nucleophilic attack.

Nucleophilic attack has been reported with small nucleophiles such as: [OH]$^-$,[9] [OR]$^-$,[9] and [NH$_2$]$^-$.[1,17] The results of murine biodistribution experiments for liposomally

encapsulated $[n\text{-}B_{20}H_{18}]^{2-}$ anion and its corresponding photoisomer, the $[i\text{-}B_{20}H_{18}]^{2-}$

anion, were compared with the hydrolysis product, the $[B_{20}H_{17}OH]^{4-}$ anion.[9] The

experiments exhibited the rapid clearance of the hydrolysis product from all tissues and

the relative retention of the two isomers. Although both isomers had tumor to blood

boron ratios above 3 at the end of the experiment, the photoisomer was retained the

longest and had the best tumor to blood boron ratio. The higher retention of the

photoisomer is consistent with the known reactivities of the two isomers since the

photoisomer undergoes nucleophilic attack at a much higher rate.[9]

The second mechanism involves the oxidation of the polyhedral borane anion to

produce a more reactive form *in vivo* (**Scheme II**).[13]
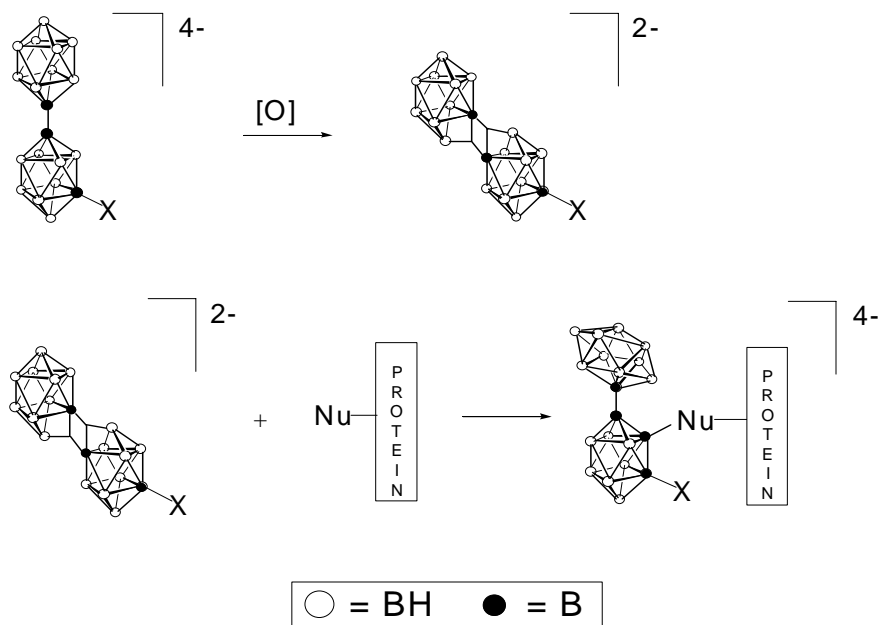
Scheme II: Proposed mechanism of retention by oxidation.

The biodistribution of the liposomally encapsulated $Na_3[ae-B_{20}H_{17}NH_3]$ exhibited an increased accumulation of boron in the tumor, up to 30 hours, and a tumor to blood boron ratio of above 3 at the end of the experiment. The low boron concentrations of $Na_3[B_{20}H_{19}]$, an anion of equal charge, and $Na_4[a e-B_{20}H_{17}OH]$,[13] an anion of similar substitution pattern, dismissed retention of $Na_3[ae-B_{20}H_{17}NH_3]$ due to anionic charge or the location of the substituent on the boron cage. The amino functionality of $[B_{20}H_{17}NH_3]^{3-}$ as a mechanism of retention was also assessed by the evaluation of liposomally encapsulated $[2-NH_3B_{10}H_9]$ in a murine biodistribution experiment.[13] The biodistribution data exhibited high boron concentrations initially, but ultimately rapid clearance from all tissues. The mechanism of retention of the $[ae-B_{20}H_{17}NH_3]^{3-}$ remained unexplained until the half-peak oxidation potentials of the polyhedral borane compounds used in the murine distribution experiments were determined. Both isomers of the $[a^2-B_{20}H_{17}NH_3]^{3-}$ ion could be oxidized more easily than any other ion investigated. Once oxidized, the resulting species, the $[B_{20}H_{17}NH_3]^-$ ion, would be susceptible to nucleophilic attack, analogous to the $[B_{20}H_{18}]^{2-}$ ions.

The final mechanism involves the bonding of thiols to form disulfide bonds (**Scheme III**).[15] Two compounds that have the potential to form disulfide bonds are $K_4[a^2-B_{20}H_{17}SH]$ and $Na_2[B_{12}H_{11}SH]$, the latter of which is currently being used in human BNCT trials in Japan.[1] The $Na_2[B_{12}H_{11}SH]$ currently being used in the clinical trials for the treatment of *glioblastoma multiforme* is not encapsulated in unilamellar liposomes. The compound has some, small, inherent tumor selectivity which is sufficient for the trials; however, most researchers agree that a new and better compound must be identified for BNCT to be successful in the future. In liposomes, the $Na_2[B_{12}H_{11}SH]$ did

not show significant accretion, consistent with its poor performance *in vivo*.[1] However, the encapsulated $K_4[a^2\text{-}B_{20}H_{17}SH]$ exhibited boron concentrations in the tumor which increased over the entire biodistribution experiment and it appears that the boron concentration would have continued to increase if a longer biodistribution experiment was completed.[15] The compound displayed the highest concentration of boron per gram of tumor recorded with liposomal delivery and a final tumor to blood ratio well above 3. The continuous increase in concentration of the boron anion in the tumor may result from the formation of a strong covalent bond.
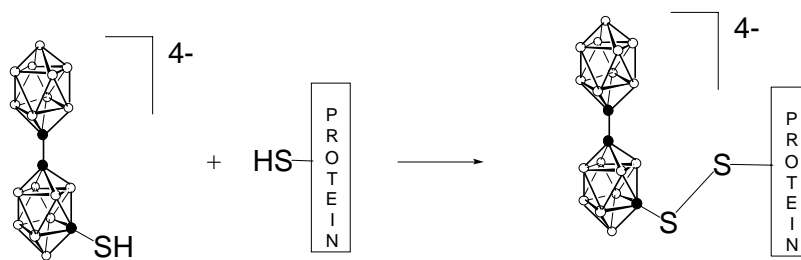
Scheme III: Proposed mechanism of retention by disulfide bond formation.

Previous studies, in and outside of our laboratory, have investigated the proposed mechanisms of binding between the polyhedral borane anions and intracellular moieties. The various methods of analysis include nuclear magnetic resonance (NMR) spectroscopy,[18] sodium dodecylsulfate polyacrylamide gel electrophoresis (SDS-PAGE),[19] dithiobisnitrobenzoic acid (DTNB),[20] capillary zone electrophoresis (CZE),[20] high performance liquid chromatography (HPLC),[20] and matrix assisted laser desorption ionization time of flight (MALDI-TOF) mass spectrometry.[20] A mixture of BSH and one of three major serum albumins (bovine, human, and dog) were analyzed with ^{11}B NMR

spectroscopy. The researchers anticipated a shift in the boron signal if a covalent bond had formed. There was no shift observed; however, the peak significantly broadened in each of the reaction spectra. Titration and variable temperature NMR were also used. Neither experiment could verify the existence of covalent interactions; however, both experiments yielded results consistent with the existence of non-covalent interactions. The existence of the non-covalent binding between BSH and the albumins is consistent with the rapid clearance of the compound observed in the murine biodistribution studies. Other experiments, using a combination of SDS-PAGE and ICP-AES were used to evaluate the potential covalent binding of specific polyhedral borane anions ($[n\text{-}B_{20}H_{18}]^{2-}$, $[a^2\text{-}B_{20}H_{17}SH]^{4-}$, and $[B_{20}H_{19}]^{3-}$) with cytochrome-C, ß-galactosidase, α-mannosidase and G-actin.[19] The proteins were selected for their abundance and location in the tumor mass, not according to the existence of specific side chain residues. After the reaction of each protein and each polyhedral borane anion was completed, a SDS-PAGE of the reaction mixture was performed. The protein spots were excised and analyzed using ICP-AES to determine the amount of boron bound to the protein (µg B/g sample). The analysis showed a high boron content for the reactions of $[n\text{-}B_{20}H_{18}]^{2-}$ and $[a^2\text{-}B_{20}H_{17}SH]^{4-}$ with α-mannosidase, and the reaction of $[a^2\text{-}B_{20}H_{17}SH]^{4-}$ and $[B_{20}H_{19}]^{3-}$ with ß-galactosidase and BSA. The location and mechanism was not evaluated. The most recent investigation to evaluate the potential binding of the polyhedral borane anions to a serum protein attempted to explain the phenomenon using SDS-PAGE, the DTNB reaction, MALDI-TOF mass spectrometry, CZE, and HPLC to evaluate binding between HSA, or BSA, and three polyhedral borane anions previously evaluated in the murine biodistribution studies, $[n\text{-}B_{20}H_{18}]^{2-}$, $[a^2\text{-}B_{20}H_{17}SH]^{4-}$, and $[ae\text{-}B_{20}H_{17}OH]^{4-}$.[20] The SDS-

PAGE experiments analyzed the reactions of BSA with each of the polyhedral borane anions. Each reaction was treated with and without dithiothreitol (DTT) to detect the presence of a covalent bond between the BSA and any of the polyhedral borane anions. The experiments resulted in an inability to detect any change in weight due to a lack of resolving capacity of the gel. The gel electrophoresis was also unable to detect ionic association because of the use of sodium dodecylsulfate (SDS) and DTT as detergents and reducing agents, respectively. The DTNB experiments are based on the reaction depicted in **Scheme IV**.
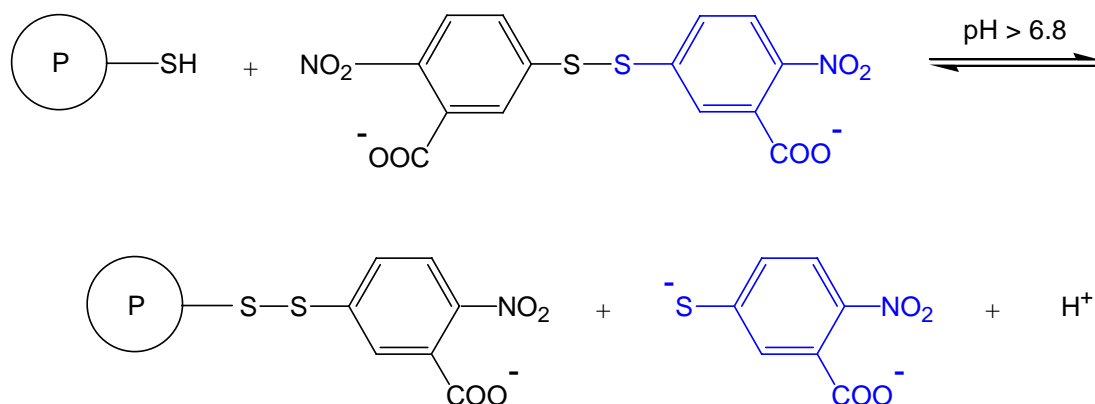
Scheme IV: Reaction of DTNB and a sulfhydryl group.

When the free thiol of DTNB binds covalently with the free thiol of another compound, forming a disulfide bond, a monomer is produced which absorbs light at a different wavelength than the original DTNB molecule.[21] After the reaction of BSA with each individual polyhedral borane anion, DTNB was added and allowed to react. If a covalent interaction occurred between the borane anion and the BSA at the free thiol of the BSA, the DTNB would not be able to bind to the thiol of BSA. As a result, no absorbance

would be observed at the new wavelength. The results for the experiment clearly demonstrated that the $K_4[a^2\text{-}B_{20}H_{17}SH]$ anion did react with the thiol moiety of the BSA; however, the results obtained for the $[ae\text{-}B_{20}H_{17}OH]^{4-}$ and $[n\text{-}B_{20}H_{18}]^{2-}$ anions were problematic. Although the $[n\text{-}B_{20}H_{18}]^{2-}$ anion is capable of reacting with the nucleophilic thiol residue to form a covalent bond, the $[ae\text{-}B_{20}H_{17}OH]^{4-}$ ion exhibits no known reactivity under physiological conditions. As a result, no absorption at the new wavelength should be observed for the $[ae\text{-}B_{20}H_{17}OH]^{4-}$ ion. This was not the case, even though a trend consistent with the reactivity of the anions was observed.

The analysis of the $K_4[a^2\text{-}B_{20}H_{17}SH]$, $Na_4[ae\text{-}B_{20}H_{17}OH]$, and $Na_2[n\text{-}B_{20}H_{18}]$ reactions with HSA by MALDI-TOF mass spectrometry exhibited significant increases in mass for all three ions. The number of anions bound to the HSA in each experiment was greater than the theoretical predictions for binding with each of the three anions. Although, in the case of the $[n\text{-}B_{20}H_{18}]^{2-}$ ion, the result could be explained by the reaction with many nucleophilic sites, the large increase in mass associated with the $[a^2\text{-}B_{20}H_{17}SH]^{4-}$ and $[ae\text{-}B_{20}H_{17}OH]^{4-}$ ions remains unexplained. The CZE and HPLC experiments showed a difference in elution time and peak broadening in the spectrum obtained from the products of the reactions between HSA and $K_4[a^2\text{-}B_{20}H_{17}SH]$ and HSA and $Na_2[n\text{-}B_{20}H_{18}]$. The largest difference in elution time in both CZE and HPLC was exhibited in the reaction products of HSA and $K_4[a^2\text{-}B_{20}H_{17}SH]$. The difference in elution time is consistent with association of the HSA and the polyhedral borane compound, and the peak broadening is potentially due to the binding of multiple polyhedral borane ions. The association was attributed to either covalent or ionic interactions. The nature and the location of the interaction between the $[a^2\text{-}B_{20}H_{17}SH]^{4-}$ and $[n\text{-}B_{20}H_{18}]^{2-}$ ions and the

serum albumins is still uncharacterized. An enhanced understanding of the mechanism(s)

of the retention for the polyhedral borane anions would improve the ability to design

future compounds with a highly probability of success for application in BNCT.

2.0 STATEMENT OF PROBLEM

BNCT is an alternative cancer treatment that is presently being evaluated. The use of BNCT is unique due to the fact that it requires no surgery and a single low dose radiation treatment. The treatment is specifically designed for aggressive forms of cancer, such as *glioblastoma multiforme*, but can, in theory, be applied to all forms of cancer. BNCT requires a boron-containing compound capable of being localized in the tumor cell. The area where the cancer is present is irradiated, causing an energetic reaction between the boron-10 isotope and the neutron. The energy from the reaction is sufficient to cause death to the tumor cell. The use of unilamellar liposomes has proven effective in delivering polyhedral borane anions into tumor cells, but the mechanism of retention remains unknown.

Although the mechanism(s) of retention are unknown, the retention has been attributed to the formation of covalent bonds with intracellular moieties, namely proteins. The polyhedral borane ions could potentially associate through ionic or covalent bonds. The use of ^{11}B NMR spectrometry, SDS-PAGE, CZE, HPLC, MALDI-TOF mass spectrometry, and DTNB probe experiments have been explored in elucidating the mechanism(s) of retention. Each of the experiments has lacked a definitive answer.

The ^{11}B NMR experiments of BSH and various albumins resulted in confirmation of ionic interactions, which was consistent with the results obtained in the murine biodistribution trials. The use of SDS-PAGE coupled with ICP-AES analyzed the

association of polyhedral borane anions with various ubiquitous cancer proteins. Associations were present, but the mechanism of binding was not determined. The CZE, HPLC, MALDI-TOF mass spectrometry, and DTNB experiments all used HSA or BSA to analyze the possible interactions of the reaction mixtures. The CZE, HPLC, and MALDI-TOF mass spectrometry experiments concluded that, while the interactions may have been stronger than expected, the interaction could not be identified as covalent or ionic in nature. The DTNB probe experiments resulted in the determination of covalent bond formation between HSA and the $[a^2\text{-}B_{20}H_{17}SH]^{4-}$ through a disulfide bond, but also produced partial binding for the physiologically unreactive borane anion. The results of these experiments do not define the nature or location of the association and further research is required to answer these questions.

The proposed research is based on an investigation of three polyhedral borane anions, $Na_2[n\text{-}B_{20}H_{20}]$, $K_4[a^2\text{-}B_{20}H_{17}SH]$, and $Na_4[ae\text{-}B_{20}H_{17}OH]$, selected based on the retention times observed in the murine biodistribution trials[8,11,13] and previous work within our laboratory. All of the anions were delivered to the tumor by liposomal delivery, but only $Na_2[n\text{-}B_{20}H_{18}]$ and $K_4[a^2\text{-}B_{20}H_{17}SH]$ were retained at a minimum boron concentration ratio of 3:1 tumor to normal tissue ratio. The $K_4[a^2\text{-}B_{20}H_{17}SH]$ was not only retained, but increased in concentration in the tumor over time. Both the $Na_2[n\text{-}B_{20}H_{18}]$ and $K_4[a^2\text{-}B_{20}H_{17}SH]$ have the potential to bind covalently at any nucleophilic sites or at the free thiol site, respectively. A comparison will be made with the two compounds and $Na_4[ae\text{-}B_{20}H_{17}OH]$, a compound with no potential for covalent binding, but which exhibited electrostatic interactions in previous studies. The research project is based on the reactions of each polyhedral borane anion with cysteine, reduced

glutathione, and human serum albumin (HSA). The binding will be analyzed using NMR spectroscopy, both SDS and native PAGE, and both ESI and MALDI mass spectrometry.

The NMR spectroscopy experiments differ from previous analyses in that amino acids and peptides will be used as small model compounds instead of serum albumin. Additionally, all previous NMR experiments utilized BSH; whereas, the current project will use $K_4[a^2\text{-}B_{20}H_{17}SH]$. In the ^{13}C NMR spectrum, a shift in the carbon signal for the carbon connected to the sulfhydryl group should be observed if the binding is covalent in nature. The COSY and HETCOR experiments will help to confirm the assignments of the carbon atoms in the ^{13}C NMR spectrum.

Although gel electrophoresis has been used previously, this project will be using native PAGE, eliminating the SDS and reducing agents from the process. As a result, native PAGE will be used to determine the presence of interactions because the proteins will migrate by both charge and molecular weight. There should be a difference in the migration of the unreacted HSA when compared to the products of each of the polyhedral borane anions reacted with HSA, if strong binding has occurred.

The mass spectrometry experiments will consist of ESI and MALDI-TOF analysis of reaction mixtures. The ESI mass spectrometry will be used to analyze the products obtained from reduced glutathione and cysteine reactions with the polyhedral borane anions. The result will be used to confirm the identity of the reaction products and is preferable to other techniques because of the soft ionization of the ESI method. The MALDI-TOF analysis will be completed after an unreduced tryptic digest is completed to detect any change in the mass of the fragments. A change in the mass of the fragment containing the free thiol from the intact protein will be used to prove the existence and

location of the covalent binding. The research project will provide additional information regarding the mechanisms of reaction and retention and should increase the accuracy of the reaction model. A better understanding of the mechanism(s) would aid in narrowing the design and synthesis of drug candidates for future application in BNCT.

3.0 MATERIALS AND METHODS

3.1 Synthesis

Materials. The polyhedral borane starting materials for the synthesis of $K_4[a^2\text{-}B_{20}H_{17}SH]$, $(Et_3NH)_2[B_{10}H_{10}]$ and $(Et_3NH)_2[n\text{-}B_{20}H_{18}]$ were prepared by previous researchers using literature procedures.[21,22-24] The Benders Salt, $KSC(O)OC(CH_3)_3$, was prepared by previous researchers using reported procedures.[25] Solutions of the $Na_2[n\text{-}B_{20}H_{18}]$ (361mM) and $Na_4[ae\text{-}B_{20}H_{17}OH]$ (272mM) compounds were prepared in deionized water by previous researchers according to literature methods.[21,22-24] Solutions for the electrophoresis experiments were obtained from Invitrogen and were used according to protocol. All other chemicals were obtained from Sigma Aldrich Chemical Company (St. Louis, Mo) and used as received, unless otherwise specified.

Measurements. The ^1H, ^{13}C, and ^{11}B Fourier transform NMR spectra were obtained at frequencies of 400 MHz, 100 MHz, and 128 MHz, respectively, using a Varian INOVA instrument. All boron spectra were obtained using quartz tubes. The residual protons of the solvents were used as the reference for chemical shifts in the proton spectra. The carbon spectra were referenced to the standard shift of acetonitrile, added as an internal reference. An external reference of $BF_3 \bullet Et_2O$ in C_6D_6 was used for the boron chemical shifts; negative values were assigned to all peaks upfield of the reference. The IR spectra were obtained using a Perkin-Elmer 1300 instrument as Nujol mulls. All spectra matched known literature values for the compounds utilized.

Preparation of K$_4$[B$_{20}$H$_{17}$SH]. (Et$_3$NH)$_2$[n-B$_{20}$H$_{18}$] (1 g, 2 mmol), Bender's Salt,

K[SC(O)OC(CH$_3$)$_3$] (2.4 g, 0.014 mol) and butylated hydroxytoluene (BHT ,0.4 g) were

placed into a 250 mL Schlenk flask. The flask was closed with a septum and purged with

argon. After the addition of 40 mL of freshly distilled THF by syringe, the reaction was

allowed to stir for 9 days under positive argon pressure. The reaction was filtered under

argon and the solid was dissolved in 50 mL deionized water at 40 °C and absolute

ethanol was added until the solution became slightly cloudy. The solution was allowed to

return to room temperature and then placed at -2 °C overnight. The solution was filtered

and the solid dissolved in 20 mL HCl (1M) to remove the protecting group. The solution

was diluted with 20 mL deionized water, and the solution was brought to boil. While

boiling, KOH (1M) was added until the solution reached a pH 10. After attaining the

proper pH, the solution was filtered while still hot to remove black particulates. The

filtered solution was returned to boiling and absolute ethanol was added until the solution

was slightly cloudy. The mixture was cooled to room temperature before being placed at

-2 °C for 3 days. The solution was filtered under positive argon pressure and the solid

was washed with six 30 mL aliquots of cold absolute ethanol. The solid was dried and

weighed to give a crude yield of 1.0 g. The first crop of K$_4$[a^2-B$_{20}$H$_{17}$SH] was mixed in

absolute ethanol for 4 hours and filtered under argon and dried to give 0.87 g (91%

yield). The solid was analyzed by ^{1}H, ^{13}C, and ^{11}B NMR to confirm the production of

K$_4$[a^2-B$_{20}$H$_{17}$SH].

Reactions of Polyhedral Borane Anions with Cysteine. Each reaction mixture

consisted of 12 mg (76.4 µmol) of cysteine and a ten fold molar excess of the polyhedral

borane anion. The reaction was dissolved in 1 mL deionized water and allowed to react at

37 ° C for 36 hours. The cysteine samples were lyophilized and reconstituted in D_2O for NMR analysis. While still in dry form, 1 mg was removed and reconstituted in 1mL 60:40 MeOH:dH_2O and 0.01% formic acid for ESI mass spectrometric analysis.

Reactions of the Polyhedral Borane Anions with Reduced Glutathione. Each reaction mixture consisted of 12 mg (39.1 μmol) of reduced glutathione and a ten fold molar excess of polyhedral borane anion. The reaction was dissolved in 1 mL deionized water and allowed to react under at 37 ° C for 36 hours. The reduced glutathione samples were lyophilized and reconstituted in D_2O for NMR analysis. While still in dry form, 1 mg was removed and reconstituted in 1 mL 60:40 MeOH:dH_2O and 0.01% formic acid for ESI mass spectrometric analysis.

Reactions of the Polyhedral Borane Anions with Human Serum Albumin. The first SDS-PAGE experiment contained two reaction mixtures which consisted of 12 mg (181 nmol) of HSA and both were reduced by treatment with DTT and denatured by incubation at 95 ℃ for 30 minutes. The DTT was removed from one of the reactions by using Microcon® Centrifugal Filter Units received from Millipore (Billerica, MA). Both the filtered and unfiltered samples containing the HSA were allowed to react with a ten fold molar excess of the $[a^2\text{-}B_{20}H_{17}SH]^{4-}$ ion for 36 hr at 37 ℃. Two control samples were treated like the others but did not contain any of the polyhedral borane ions. One of the controls was stored at 4 ° C immediately after being denatured. At the end of 36 hours, all samples were placed at 4℃ until analysis with SDS-PAGE.

The second SDS-PAGE experiment contained 12 mg (181 ηmol) of HSA. Both samples were reduced by treatment with DTT and denatured by incubation at 95 ℃ for 30 minutes. One of the samples was immediately frozen after being reduced and

denatured, while the other sample was allowed to react for 36 hr at 37 º C without any polyhedral borane ions. At the end of 36 hours, both samples were place at 4°C until analysis with SDS-PAGE.

The native PAGE consisted of 12 mg (1.8 ηM) of HSA and a ten fold molar excess of the polyhedral borane anion. The reaction mixture was dissolved in 1 mL deionized water and allowed to react for 36 hours at 37 º C. A control containing 10 mg of HSA with no polyhedral borane anion was treated in an identical manner. After 36 hours, the reaction mixtures were placed at 4°C until needed.

3.2 Instrumental Analysis

Nuclear Magnetic Resonance Spectroscopy. Before analyzing any of the reaction mixtures, controls were performed on each of the starting materials and on each of the solvents to detect for possible contaminants. Stock solutions of reduced glutathione, oxidized glutathione, cysteine, and cystine were analyzed by ^{1}H, COSY, ^{13}C, and HETCOR experiments, in 1 mL D_2O as solvent. Each one-dimensional ^{1}H NMR spectrum was referenced to the residual water peak (4.6 ppm) and COSY analysis was completed to detect the proton coupling. After the COSY experiment was completed, three drops of acetonitrile were added as a reference for the ^{13}C NMR spectra. The acetonitrile reference was determined by its relevant position to 3-(trimethylsilyl-1-propanesulfonic acid in D_2O.

ESI Mass Spectrometry. All samples were evaluated on a Finnigan MAT LCQ mass spectrometer. The samples were injected at a flow rate of 10 μL/minute with a 3.5 kV spray voltage and a 200 μA spray current. The capillary was heated to 220 ºC and a

sheath gas flow rate of 45 arb was set. The spectra were analyzed using Xcalibur

software. Each spectrum represents an average signal intensity over time. Each of the

polyhedral borane anions and the reduced glutathione were analyzed as standards.

Afterwards, the mass spectrum of the individual reaction mixtures of reduced glutathione

with $Na_2[n$-$B_{20}H_{18}]$, $K_4[a^2$-$B_{20}H_{17}SH]$, and $Na_4[ae$-$B_{20}H_{17}OH]$, were obtained for

comparison with the results obtained with the standard compound.

SDS-PAGE. Each reaction mixture of unfiltered and filtered denatured HSA with

$Na_4[a^2$-$B_{20}H_{17}SH]$ was loaded into 10% Tris-HCl running gel with a 4% stacking gel.

The unreduced samples were placed in native sample buffer (0.5 M Tris-HCL, pH 6.8,

glycerol, 0.05% bromophenol blue) before being loaded into the gel. The reduced

samples were placed in sample buffer (2% SDS, 0.5 M Tris-HCL, pH 6.8, glycerol,

0.05% bromophenol blue) before being loaded into the gel. Each sample load was at a

total volume of 25 µL in each well. The wells of lane 2-5 were loaded with unreduced

reaction mixtures, while the wells of lanes 6-9 were loaded with the reduced samples of

the same reaction mixtures. A second SDS-PAGE experiment was performed to compare

the HSA sample that was frozen after being denatured with the HSA sample that was

treated with no polyhedral borane ions, but incubated under the same conditions as the

reaction mixtures of the first SDS-PAGE experiment. Each well received 1 µL (10 µg) of

each reaction mixture. The gel was placed in an Invitrogen rig with Tris-Glycine buffer

and was left at 150 Volts for 1.5 hours. After that time, the gel was stained with Simple

Blue stain and photographed using Kodak Imager software.

Native PAGE. Each reaction of HSA with $Na_2[n$-$B_{20}H_{18}]$, $K_4[a^2$-$B_{20}H_{17}SH]$ and

$Na_4[ae$-$B_{20}H_{17}OH]$ was placed in a lane of a 3-8% NuPage Tris-Acetate gel. Pierce

Chemiluminescent Blue Ranger was used as the molecular weight ladder. An aliquot of 10 μL (100 μg) was removed from each reaction mixture and treated with native gel buffer (0.5 M Tris-HCl, pH 6.8, glycerol, 0.05% bromophenol blue) giving a total volume of 25 μL in each well. The gel was placed in an Xcell with Tris-Acetate buffer (Invitrogen) and was left at 1.5 V for 6 hr. After that time, the gel was stained use Simple Blue stain and photographed using Kodak Imager software.

MALDI-TOF Mass Spectrometry. Before analysis on the MALDI-TOF mass spectrometer, a tryptic digest was performed on a 20 μg sample that was removed from the HSA and $K_4[a^2\text{-}B_{20}H_{17}SH]$ stock reaction mixture. A 20 μg sample of unreacted HSA was also evaluated as a reference. The samples were filtered using Microcon® Centrifugal Filter Units received from Millipore (Billerica, MA) and then lyophilized and reconstituted in a digestion solution containing Promega Trypsin GOLD (1:10, protease to protein), 20% acetonitrile (ACN), and 80% of a 50 mM ammonium bicarbonate buffer, pH 8). After 19 hours at 37 ºC, the reaction mixtures were removed and eluted using ZipTips. Each ZipTip was equilibrated with five volumes of ACN, elution buffer (20% ACN, 80% of a 50 mM ammonium bicarbonate buffer, pH 8, 0.01% trifluoroacetic acid (TFA)), and deionized water. The digest (10 μL) was pipetted into the ZipTip and washed with five volumes of deionized water and five volumes of elution buffer. The digest was eluted using 10 μL of ACN and expelled into a 500 μL tube. The HSA reaction and the unreacted HSA were place in separate tubes. This process was repeated with five ZipTips, all being eluted into their respective 500 μL sample tubes. The elution solutions were lyophilized and reconstituted in a α-cyano-4-hydroxycinnamic acid matrix and dried on a MALDI-TOF plate.

4.0 RESULTS AND DISCUSSION

The use of radiation and chemotherapy has proven to be ineffective in the removal of many types of highly aggressive forms of cancer. The lack of specificity and selectivity of these methods has lead to the exploration of boron neutron capture therapy (BNCT) as an alternate means of treatment. The use of BNCT is believed to be an improvement because of the minimum amount of normal cell death, which is a severe side effect of traditional treatment protocols and is important in the treatment of brain cancers such as *glioblastoma multiforme*. BNCT has also been used in treatment of metastic melanoma and could potentially be used to treat a wide variety of cancers. The efficacy of the treatment is dependant on the selective localization and retention of the boron-containing compounds in the interior of tumor cells. Effective retention is evaluated by the ratio of the concentration of the boron in the tumor to the concentration of the boron in the normal tissue. The ideal ratio is a minimum of 5:1. Once the compound has localized in the tumor, the tumor area is irradiated with neutrons, a type of radiation with a relatively low ability to harm normal tissue. The neutrons cause a fission of the resulting boron isotope, producing sufficient energy to destroy the cells of the tissue containing the boron.

The predominance of the current research in BCNT is based upon two compounds: sodium borocaptate (BSH), which contains 12 boron atoms, and *p-*

boronophenyalanine (*p*-BPA), which only contains one boron atom. The research performed by our laboratory, both past and present, have used compounds that contain 20 boron atoms, primarily $Na_2[n\text{-}B_{20}H_{18}]$, $K_4[a^2\text{-}B_{20}H_{17}SH]$, and $Na_4[ae\text{-}B_{20}H_{17}OH]$. The advantage of using compounds that contain more boron atoms is that a smaller amount of the compound is required to obtain the same dose.

The polyhedral borane anions were selected based on their known reactivity and retention, or lack of retention, as liposomally encapsulated compounds in the tumor during murine biodistribution studies. The $Na_2[n\text{-}B_{20}H_{18}]$ and $Na_4[a^2\text{-}B_{20}H_{17}SH]$ both showed retention in the tumor over time in comparison with normal cells, but $K_4[a^2\text{-}B_{20}H_{17}SH]$ also exhibited an increase in concentration throughout the time course experiment. The $Na_4[ae\text{-}B_{20}H_{17}OH]$ was cleared from the tumor cells and will be used as a control for the reactions. The retention of $K_4[a^2\text{-}B_{20}H_{17}SH]$ and $Na_2[n\text{-}B_{20}H_{18}]$ is believed to result from the formation of a covalent bond with the nucleophilic sites on proteins in tumor cells. In the case of the $Na_4[a^2\text{-}B_{20}H_{17}SH]$, the target would be a thiol substituent on a cysteine residue whereas, in the case of $Na_2[n\text{-}B_{20}H_{18}]$, any nucleophilic site could potentially suffice. Previous research in our laboratory evaluated the reactions of HSA and BSA with $Na_2[n\text{-}B_{20}H_{18}]$, $K_4[a^2\text{-}B_{20}H_{17}SH]$, $Na_4[ae\text{-}B_{20}H_{17}OH]$, and $Na_3[B_{20}H_{19}]$. The analysis of the reactions of the first three compounds, of primary interest to the current project, and albumins were examined using HPLC, CZE, a DTNB probe, and MALDI-TOF mass spectrometry. The HPLC and CZE experiments with $Na_2[n\text{-}B_{20}H_{18}]$ and $K_4[a^2\text{-}B_{20}H_{17}SH]$ with BSA resulted in an increase in the elution time when compared with the unreacted BSA. The shift in elution time is attributed to interactions between the BSA and the polyhedral borane anions. In the DTNB

experiments, HSA showed binding to $K_4[a^2\text{-}B_{20}H_{17}SH]$ at the free thiol moiety of the protein;[20] however, there was also some unexplained binding observed in the experiments with the $Na_2[n\text{-}B_{20}H_{18}]$ and $Na_4[ae\text{-}B_{20}H_{17}OH]$ anions. The binding of HSA to $Na_2[n\text{-}B_{20}H_{18}]$ was explained by possible nucleophilic attack, but the binding of the $Na_4[ae\text{-}B_{20}H_{17}OH]$, which is not reactive under normal physiological conditions, to HSA could not be explained. The MALDI-TOF experiments showed association with all of the polyhedral borane anions to the protein. Since all of the compounds were bound and the $Na_4[ae\text{-}B_{20}H_{17}OH]$ compound is known to be unreactive in aqueous solution, the compounds must, to a large extent, be associated by ionic interactions.

In summary, previous research has shown that disulfide bond formation is possible with the free thiol of BSA[20] and that various moieties on the protein structure have the ability to undergo an ionic interaction with all of the polyhedral borane anions. In order to simplify some of the complexity of the protein molecules, smaller molecules were selected for investigation and NMR, ESI mass spectrometry, native PAGE, and MALDI-TOF mass spectrometry experiments were designed in order to assist with the understanding of the nature, availability, and the location of the binding to HSA.

The amino acid cysteine was chosen because it is the simplest thiol containing biomolecule (**Figure 3**) and cysteine is also the target amino acid for binding the $[a^2\text{-}B_{20}H_{17}SH]^{4-}$ to HSA.
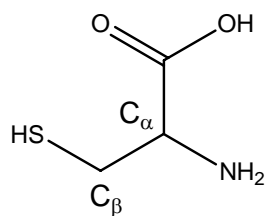

Figure 3: Structure of cysteine.

The simplicity of the cysteine structure allows a clear view of the interactions and a foundation to begin an analysis of more complex thiol-containing molecules. The oxidized form of cysteine, cystine (**Figure 4**), was selected because it is a cysteine dimer connected by a disulfide bond.
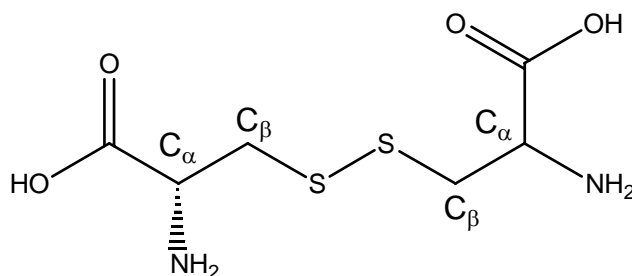
Figure 4: Structure of cystine.

The analysis of cystine can be used as a reference for disulfide bond formation and compared with the reactions of cysteine. The formation of the disulfide can be evaluated easily using a combination of NMR spectroscopy and ESI mass spectrometry.

Glutathione was selected because it is an abundant thiol-containing peptide. The presence of reduced glutathione in chemically resistant tumors and overall presence in tumor cells makes it an excellent candidate for evaluation.[27] The structure of reduced glutathione can be characterized as an α-glutamtyl (red in **Figure 5**) connected to a cysteine (black in **Figure 5**) with a glycine terminus (blue in **Figure 5**). The only location on the peptide with the ability to form a disulfide bond is the thiol residue of the cysteine. Thus, the reduced glutathione and $K_4[a^2\text{-}B_{20}H_{17}SH]$ reaction can produce a disulfide, while the reduced glutathione and $Na_2[n\text{-}B_{20}H_{18}]$ can form covalent bonds through nucleophilic attack at a variety of locations. The formation of the disulfide bond can be

evaluated by NMR and ESI mass spectrometry and compared to the oxidized glutathione (**Figure 5**).
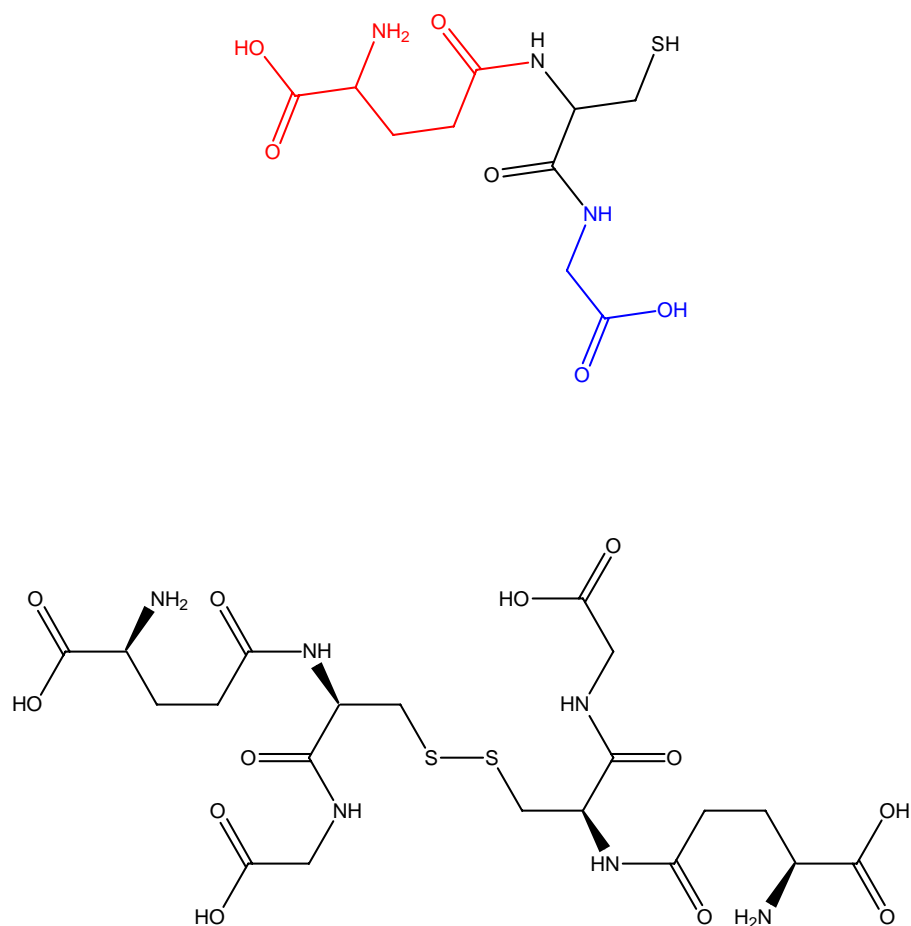
Figure 5: Structure of reduced glutathione (top) and the structure of oxidized glutathione (bottom).

Analysis of the small molecule model compounds serve as a basis for the continued analysis of HSA. HSA is a protein which contains a free thiol at cysteine-34, is well characterized, and inexpensive. The globular nature and complexity of HSA gives way to various nucleophilic sites and a variety of locations for ionic binding, an attribute which is not possible in the small molecule model compounds. The larger molecular

weight and complexity of the HSA also makes the NMR and ESI analysis more difficult due to its multiple charges and the existence of numerous carbon atoms. Instead, SDS-PAGE will be used to measure the differential migration of the reacted and unreacted protein, and MALDI-TOF mass spectrometry will be used to compare reacted and unreacted tryptic digests of the protein to determine the mass difference for specific sequences.

4.1 Synthesis and Anticipated Reactivity

Each of the polyhedral borane compounds ($Na_2[n\text{-}B_{20}H_{18}]$, $K_4[a^2\text{-}B_{20}H_{17}SH]$, $Na_4[ae\text{-}B_{20}H_{17}OH]$) were allowed to react with cysteine, reduced glutathione, and HSA at 37 °C for 36 hr in deionized water. After the allotted time period, aliquots were removed for the specific analyses, including NMR spectroscopy, ESI and MALDI-TOF mass spectrometry, and gel electrophoresis.

Cysteine (**Figure 5**) has two potentially nucleophilic sites, depending on the pH. If the $[n\text{-}B_{20}H_{18}]^{2-}$ ion reacted with cysteine, two reactions are possible. In the first reaction, the nucleophilic amino group attacks the electron-deficient bonding region in the $[n\text{-}B_{20}H_{18}]^{2-}$ ion (**Scheme V**) whereas, in the second reaction, the nucleophilic sulfhydryl group is making the attack (**Scheme VI**).
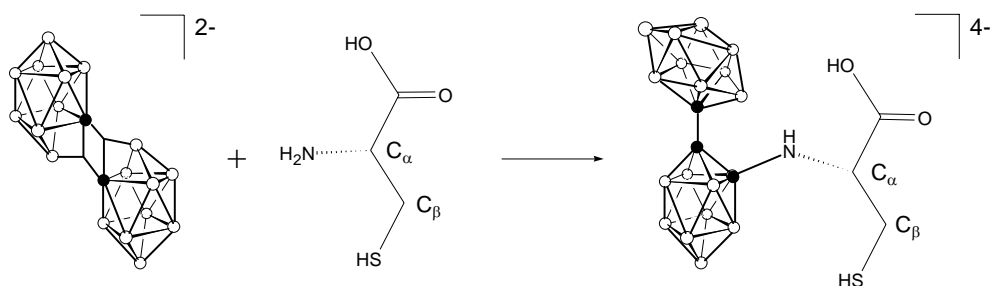
Scheme V: Reaction of the $[n\text{-}B_{20}H_{18}]^{2-}$ ion and the α-amino group of cysteine.
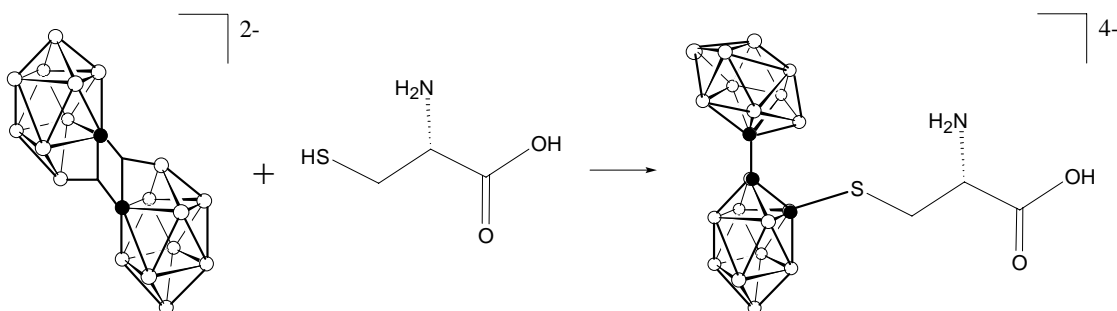
Scheme VI: Reaction of the $[n\text{-}B_{20}H_{18}]^{2-}$ ion and the sulfhydryl group of cysteine.

If the $[a^2\text{-}B_{20}H_{17}SH]^{4-}$ ion reacted with cysteine, the reaction forming the disulfide bond (**Scheme VII**) would be expected.
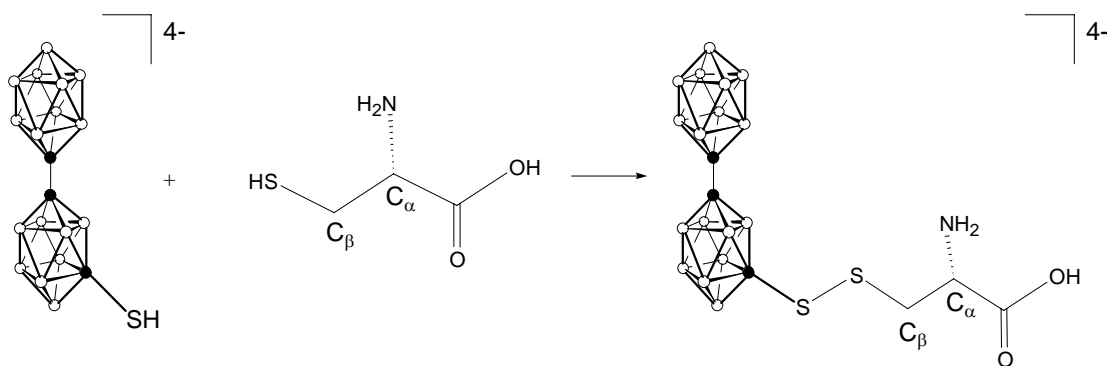
Scheme VII: Reaction of the $[a^2\text{-}B_{20}H_{17}SH]^{4-}$ ion and the sulfhydryl group of cysteine.

In reduced glutathione, the potential reaction sites for the $[n\text{-}B_{20}H_{18}]^{2-}$ ion would be at the α-amino group (**Scheme VIII**) and at the sulfhydryl group (**Scheme IX**), analogous to cysteine. The potential reactivity of both of the reaction sites is dependent on the pH of the solution. Although two other –NH groups are present in reduced glutathione, both –NH groups are part of an amide functionality and are not expected to be sufficiently nucleophilic for the anticipated reaction.
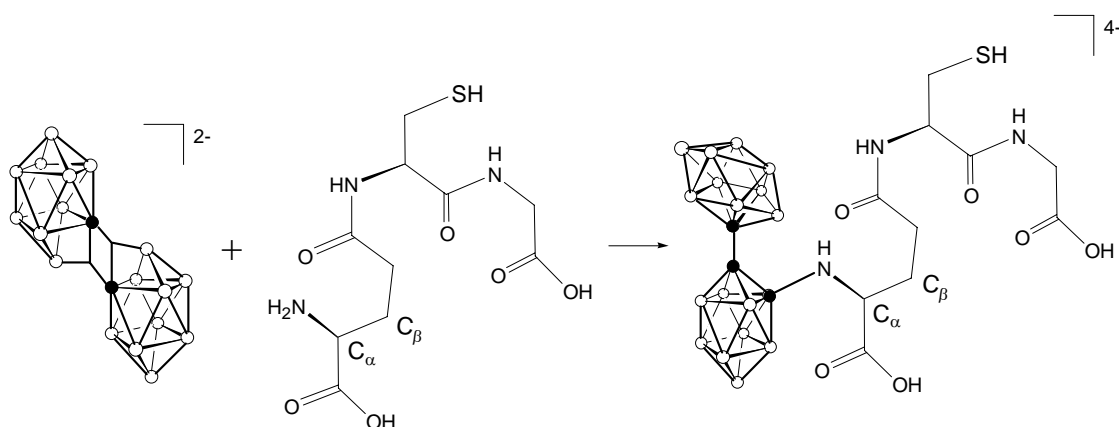
Scheme VIII: Reaction of the $[n\text{-}B_{20}H_{18}]^{2-}$ ion and the α-amino group of reduced glutathione.

The reaction of reduced glutathione with the $[a^2\text{-}B_{20}H_{17}SH]^{4-}$ ion (**Scheme IX**) would produce a disulfide bond between the two sulfhydryls of the cysteine residue and the $[a^2\text{-}B_{20}H_{17}SH]^{4-}$ ion, analogous to the cysteine reaction.
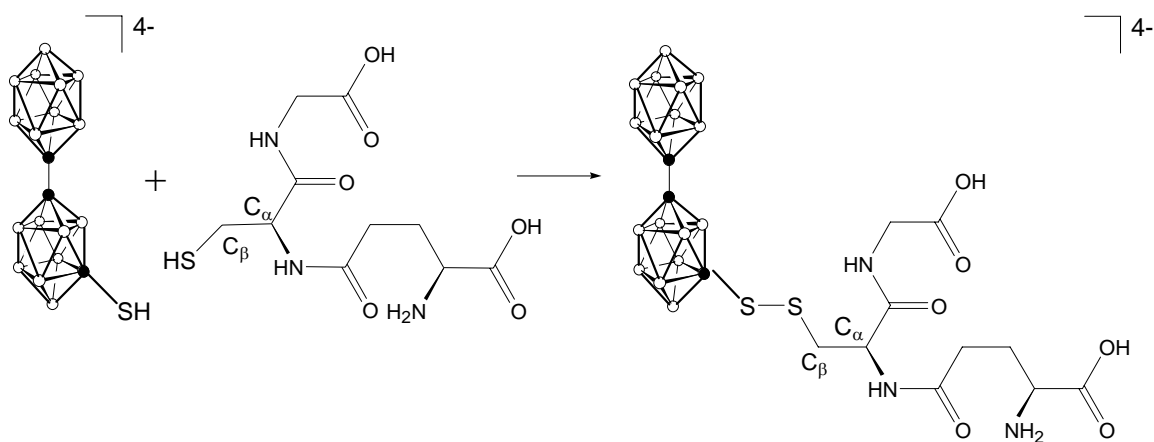
Scheme IX: Reaction of the $[a^2\text{-}B_{20}H_{17}SH]^{4-}$ ion and the sulfhydryl group of reduced glutathione.

The potential reaction sites on HSA are numerous, but can be generally characterized as any nucleophilic sites, including the free sulfhydryl group. All of the

sites are dependent on the pH of the reaction. The $[n\text{-}B_{20}H_{18}]^{2-}$ ion could potential react in a nucleophilic manner with HSA on any one of the nucleophilic sites on the globular protein (**Scheme X**).
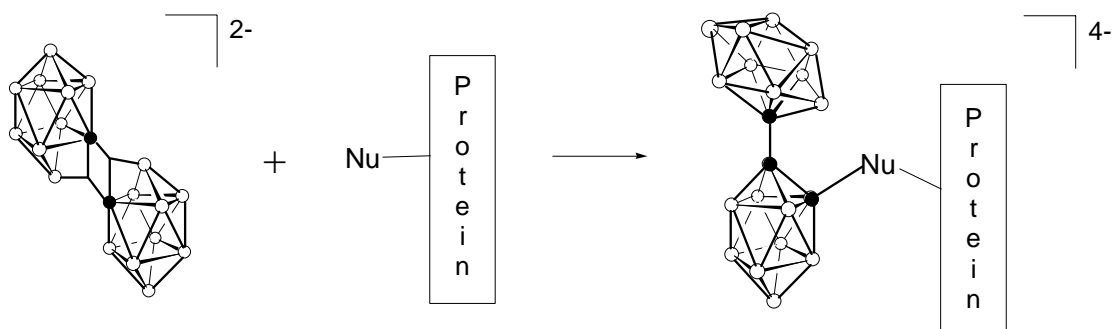
Scheme X: Reaction of the $[n\text{-}B_{20}H_{18}]^{2-}$ ion and a nucleophilic group on HSA.

However, the $[a^2\text{-}B_{20}H_{17}SH]^{4-}$ ion should only react with the free sulfhydryl group of a cysteine residue on the HSA, producing a disulfide bond (**Scheme XI**).
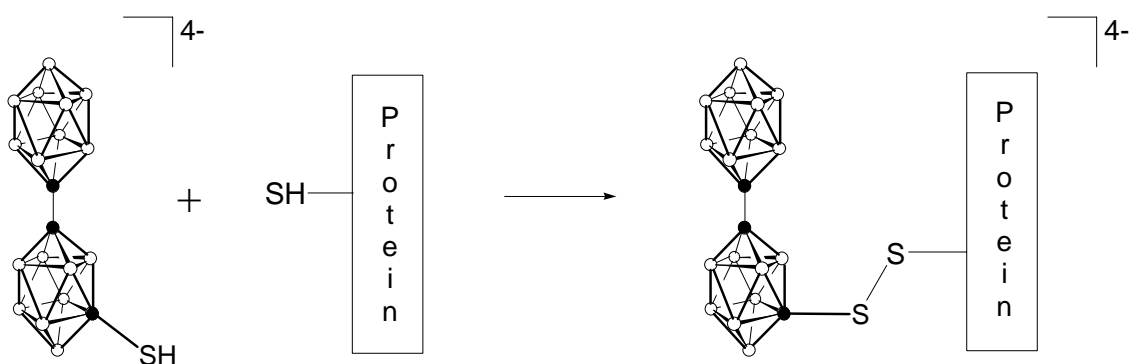
Scheme XI: Reaction of the $[a^2\text{-}B_{20}H_{17}SH]^{4-}$ ion and the sulfhydryl group of HSA.

4.2 NMR Spectroscopy

The use of one-dimensional ^{1}H and ^{13}C NMR spectroscopy, combined with COSY and HETCOR experiments, should establish the correct assignment of the carbon peaks in the obtained spectra. The COSY experiments enable correlation between neighboring protons in the compound. The correlation of the proton signal is designated by an off-diagonal contour whenever the assigned signals are protons on adjacent carbon atoms. Therefore, the coupling will establish the connectivity of the protons in the compound and enable the correct assignment of all signals in the ^{1}H NMR spectra. The HETCOR experiments enable correlation between the one-dimensional ^{1}H and ^{13}C NMR spectra. The ^{1}H NMR spectrum, on the y-axis is correlated with the ^{13}C NMR spectrum on the x-axis. The off-diagonal resonances are used to establish an association of the proton signals with their corresponding carbon signal. Evaluation of the one-dimensional ^{1}H and ^{13}C NMR, COSY, and HETCOR spectra will enable the assignment of any change in the electronic environment resulting from the covalent binding of the polyhedral borane anion.

Evaluation of the Cysteine Reaction by ^{1}H NMR Spectroscopy. The simplicity of the cysteine results in a ^{1}H NMR spectrum with only two sets of signals. As a result of the software, there is also a large wrap-around peak for the proton on H_2O at 2.48 ppm. The extra signal is not relevant to the current discussion (**Figure 6**). The triplet centered at 4.10 ppm is assigned to the protons on the α-carbon while the quartet centered at 2.90 ppm is assigned to the protons on the carbon atom adjacent to the sulfhydryl substituent, the β-carbon. The quartet and its associated fine splitting is a result of splitting by two
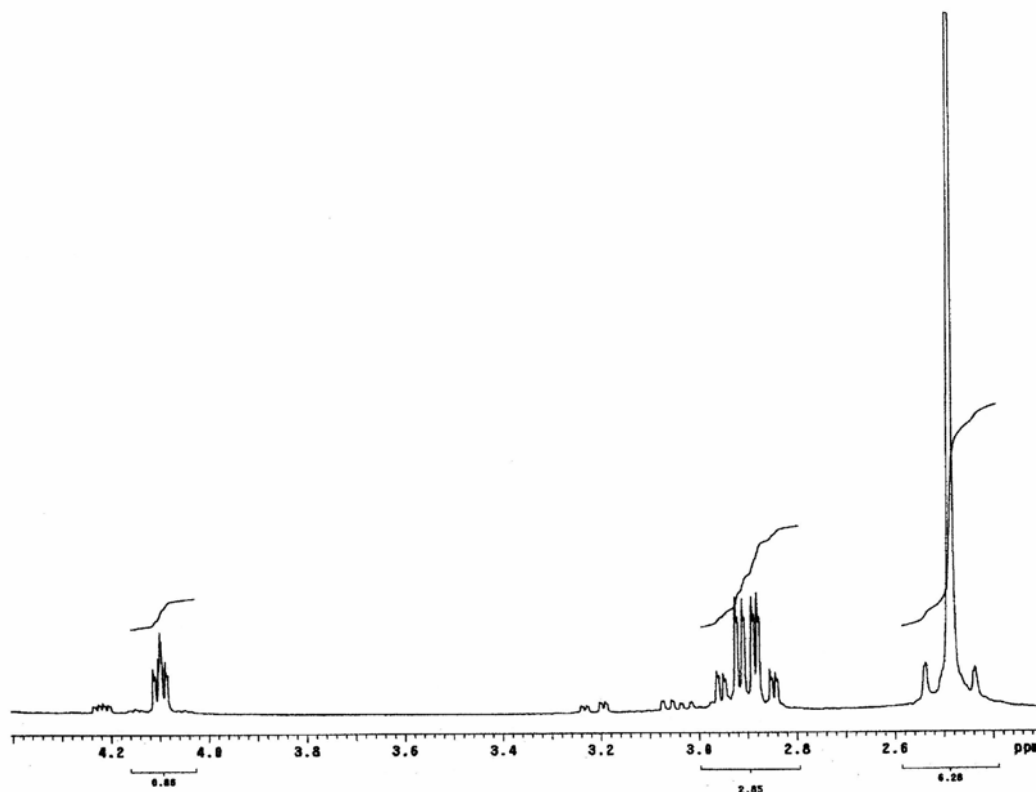
Figure 6: ^{1}H NMR spectrum of unreacted cysteine.

nuclei, the sulfur nuclei, resulting in a quartet, and the splitting of those peaks into

doublets from the proton on the α-carbon.A ^{1}H NMR spectrum of pure cystine could not

be obtained because of the large water peak resulting from the acidification required to

dissolve the powder.

Evaluation of the Cysteine Reaction by ^{13}C NMR Spectroscopy. The ^{13}C NMR

spectrum of cysteine contains four carbon signals, even though only two carbon signals

should be in the viewing window. The two peaks, at 24.3 and 54.9 ppm, are attributed to

the ß and α-carbons, respectively. No signal is observed for the quaternary carbonyl

carbon because the signal is outside of the viewing window. The other two peaks, located

at 36.2 and 53.1ppm, are from the ß and α-carbons of cystine. The two peaks are present in cysteine due to a small amount of cystine contamination or, alternatively, formation of cystine in the aqueous solution. The signal at 36.2 ppm in cystine, and lack of the signal at 24.3 ppm, is attributed to a signal shift in the ß carbons and is due to the formation of a disulfide bond (**Figure 7**). The ^{13}C NMR spectrum of the reaction of cysteine with $[a^2$-$B_{20}H_{17}SH]^{4-}$ ion result in two peaks, at 29.7 ppm and 38.5 ppm, not corresponding to cysteine or cystine.

Evaluation of the Cysteine Reaction by COSY and HETCOR NMR Spectroscopy. The COSY experiment shows the original peaks at 4.10 and 2.90 ppm on the diagonal. The existence of the cross-coupling peak, circled in the spectrum shown in **Figure 8**, indicates that the two signals correspond to the protons on adjacent carbon atoms. The results of the HETCOR experiment (**Figure 8**) show a cross-coupling peak between the triplet centered at 4.10 ppm in the ^{1}H NMR and the signal at 54.9 ppm which corresponds to a carbon atom with a single proton attached, the α-carbon. Similarly, a peak coupling is observed between the quartet in the ^{1}H NMR spectrum centered at 2.90 ppm and the signal at 24.3 ppm in the ^{13}C NMR spectrum. As a result, the carbon at 24.3 ppm corresponds to the carbon atom adjacent to the sulfur atom (**Figure 8**), the β-carbon.

The spectrum of the reaction mixture of cysteine and $K_4[a^2$-$B_{20}H_{17}SH]$ denotes two new peaks, at 36.5 ppm and 29.8 ppm which are caused by a shift in the α and ß-carbons, respectively, of the reacted cysteine. A similar shift in carbon peaks is observed in the comparison of the cysteine and cystine ^{13}C NMR spectra. Therefore, the shift of the
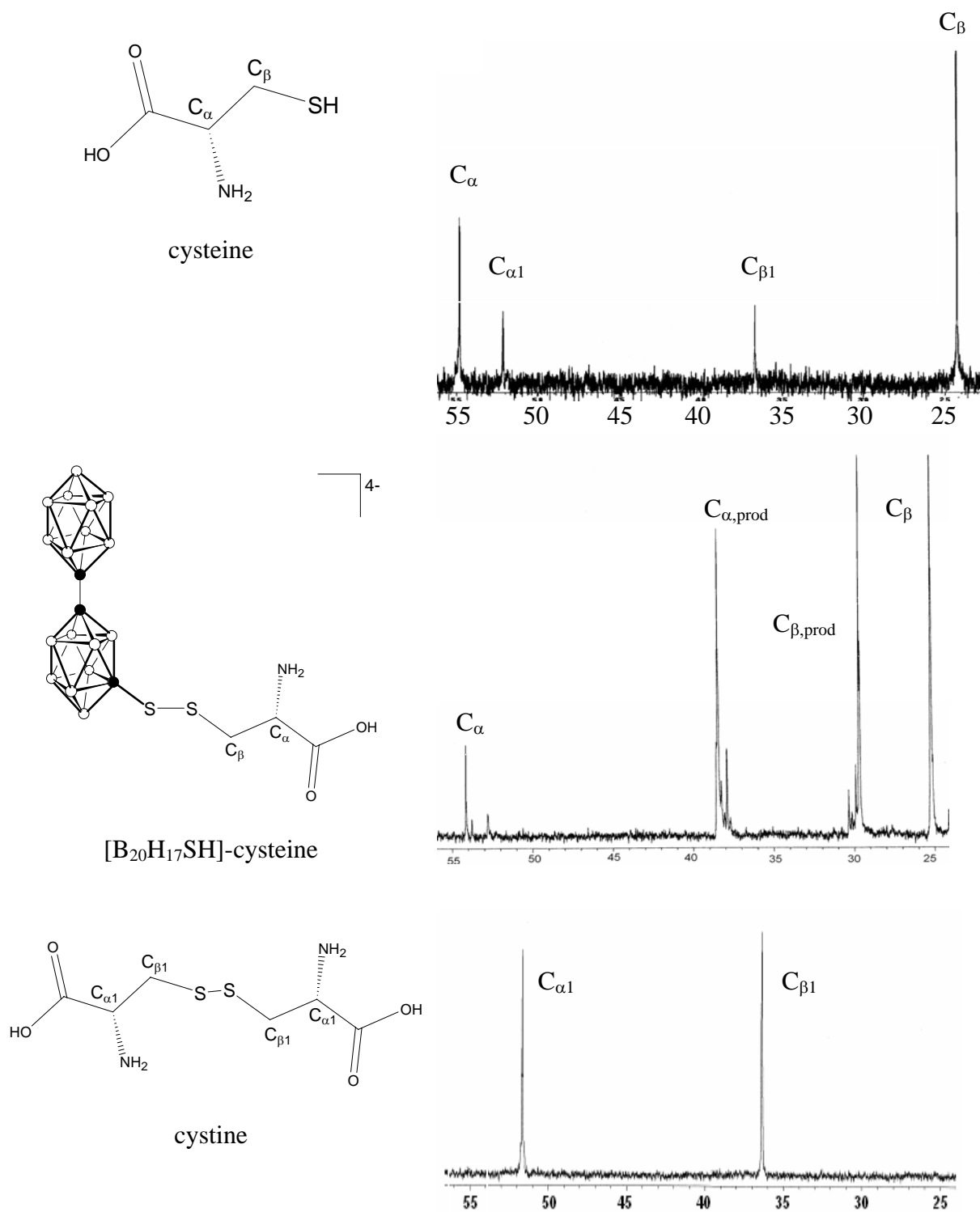
Figure 7: ^{13}C NMR spectral comparison of unreacted cysteine (top), reaction mixture of cysteine and $K_4[a^2\text{-}B_{20}H_{17}SH]$ (middle), and cystine (bottom).
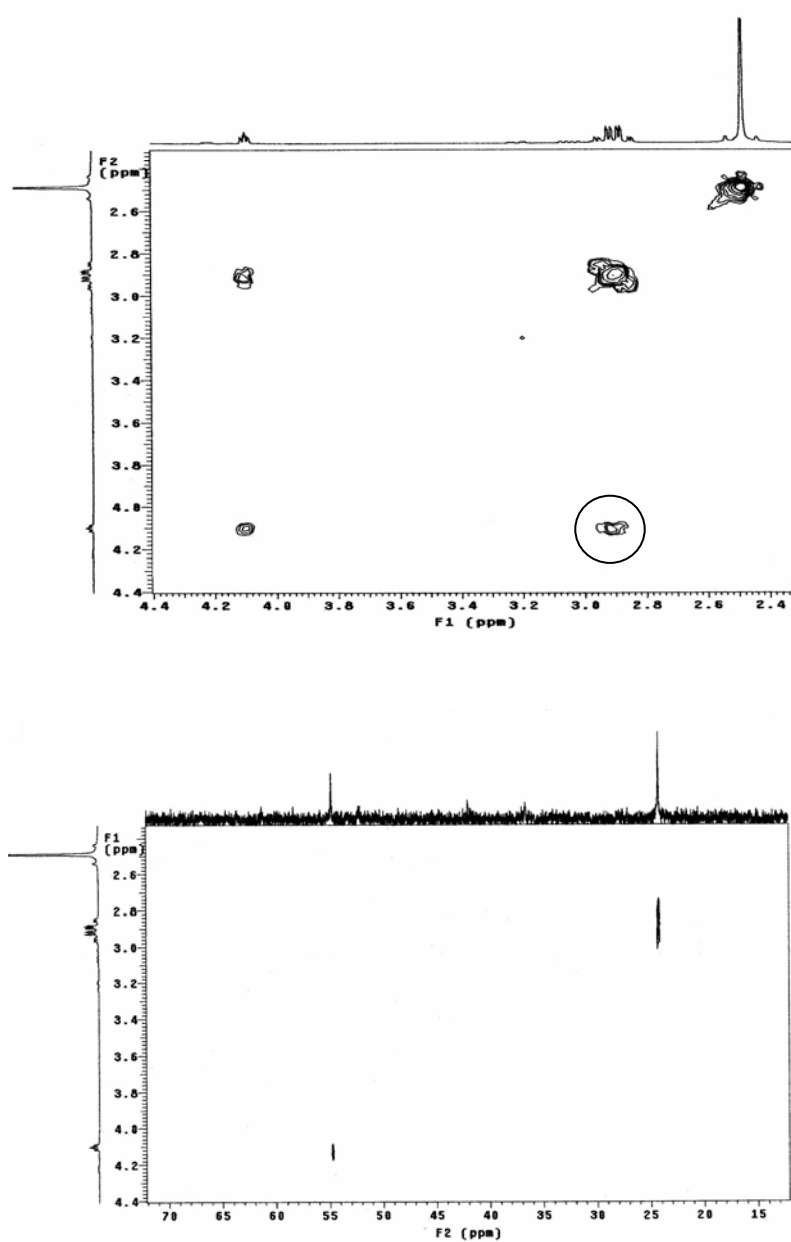
Figure 8: COSY (top) and HETCOR (bottom) of unreacted cysteine.

carbon peaks in the ^{13}C NMR spectrum of the reaction of cysteine and K$_4$[a^2-B$_{20}$H$_{17}$SH] is attributed to the formation of a disulfide bond, analogous to the ^{13}C NMR spectrum of cystine. The lack of disappearance of the peaks at 24.3 ppm and 54.9 ppm suggest that the reaction is not complete.

COSY and HECTOR experiments provide a means of unambiguously assigning peaks in the one-dimensional ^{1}H and ^{13}C NMR spectra. Although the cysteine example is uncomplicated, the COSY and HETCOR analysis serve as a basis for more complex molecular determinations.

Evaluation of the Glutathione Reactions by ^{1}H NMR Spectroscopy. The experience gathered from the evaluation of the cysteine reactions should be applicable to the reduced glutathione reactions. The potential binding sites in the reduced glutathione are the α-amino group of the glutamyl group and the sulfhydryl group of the cysteine amino acid. The nucleophilic attack by both Na$_2$[n-B$_{20}$H$_{18}$] and K$_4$[a^2-B$_{20}$H$_{17}$SH] would cause the formation of a covalent bond and would cause a shift in the carbon signal adjacent to the appropriate functional group. The formation of the disulfide bond should produce a shift in the signal assigned to the ß-carbon of the cysteine residue, which is adjacent to the free sulfhydryl, and reaction with the α-amino group should produce a shift in the signal assigned to the α-carbon of the cysteine residue.

The reduced glutathione spectra exhibits signals at 4.32 and the 2.72 ppm and are attributed to the α and ß-carbons of the cysteine residue of the reduced glutathione, respectively (**Table I**). The reduced glutathione spectra also contain signals at 1.97, 2.34, 3.63, and 3.76 ppm, which are similar to those observed in the oxidized glutathione (**Figure 9**). The similarity of the peaks is due to the presence of the unaltered glutamyl

and glycine residues of reduced glutathione. The triplet at 3.63 ppm is attributed to the proton of the α-carbon of the glutamyl residue, which is adjacent to the β-carbon atom containing two protons. The two quartets at 1.97 and 2.34 ppm correspond to the protons on the γ and β-carbons of the glutamyl residue. The protons on the γ-carbon are deshielded by the carbonyl from the amide linkage between the glutamyl and cysteine residues, resulting in the signal at 2.34 ppm. The other quartet is assigned to the protons of the β-carbon of the glutamyl residue. The singlet at 3.76 ppm results from the protons of the glycine residue. The only proton signal that experiences a significant shift, from 4.34 ppm to 4.52 ppm, is assigned to the protons of the α-carbon of the cysteine residue. The new signal at 3.06 ppm is attributed to the protons of the β-carbon of the cysteine residue adjacent to the sulfhydryl, which is where the covalent bond is formed.

Evaluation of the Glutathione Reactions by ^{13}C NMR Spectroscopy. Six peaks, at 25.3, 26.2, 29.7, 42.1, 54.7, and 55.2 ppm, are observed in the ^{13}C NMR spectrum of reduced glutathione. The less intense peaks are attributed the rotation of the carbon atoms at the glutamyl and glycine residues.[28] The peaks at 25.3 ppm and 55.7 ppm are assigned to the α and β-carbon atoms, respectively, of the cysteine residue of reduced glutathione. The peak at 26.2 ppm is assigned to the β-carbon of the glutamyl residue. The peaks at 54.7 and 29.1 ppm are assigned to the α and γ-carbons of the glutamyl residue, and the peak at 42.1 ppm is assigned to the α-carbon of the glycine residue (**Table II**). When comparing the oxidized glutathione ^{13}C NMR spectrum with the reduced glutathione ^{13}C NMR spectrum, the only significant shifts are assigned to the peaks of the carbon atoms in the cysteine residue. There is a small shift in the γ-carbon of the glutamyl residue, from 29.7 ppm to 31.2 ppm, and a significant shift in the β-carbon of the cysteine residue, from

25.3 to 39.1 ppm. The peak at 39.1 ppm is unique to the oxidized compound and is the result of a disulfide bridge. The peak at 39.1 ppm is also present in the $K_4[a^2\text{-}B_{20}H_{17}SH]$ reaction (**Figure 10**). The reaction mixtures of $Na_2[n\text{-}B_{20}H_{20}]$ and $Na_4[ae\text{ -}B_{20}H_{17}OH]$ with reduced glutathione did not produce the peak at 39.1 ppm and no significant shifts in peak locations were observed (**Figure 11**).

Table I: Comparison of ^1H NMR spectral shifts observed for cysteine, reduced glutathione, and oxidized glutathione.

	Glutamyl			Cysteine		Glycine
	α	B	Γ	α	β	γ
Cysteine (ppm)	XXXXXX	XXXXXX	XXXXX	2.90	4.10	XXXXXXX
Reduced glutathione (ppm)	3.63	1.97	2.34	4.32	2.72	3.76
Oxidized glutathione (ppm)	3.63	1.97	2.34	4.52	3.06, 2.72	3.78

Evaluation of the Glutathione Reactions by COSY and HETCOR NMR Spectroscopy. The combination of COSY and HETCOR experiments will determine proton coupling and correlate the carbon peaks with proton peaks to give an assignment of each carbon atom in the reduced glutathione and the oxidized glutathione.

The COSY spectrum for reduced glutathione contains three cross-coupling signals at 1.97, 2.32 ppm, and 3.63 ppm in the off-diagonal region. The signals are assigned to the α, β, and γ carbons of the glutamyl residue, respectively (**Figure 12**). The cross-coupling contours for these proton signals were correlated to the carbon signals at 29.1, 54.7, and 26.2 ppm with HETCOR experiments (**Figure 13**). The proton signals for the α and β carbons of the cysteinyl residue, at 2.77 and 4.34 ppm, were correlated to the

Table II: Comparison of ^{13}C NMR spectra of reduced glutathione, oxidized glutathione, and reduced glutathione reaction mixtures of $[a^2\text{-}B_{20}H_{17}SH]^{4-}$, $[n\text{-}B_{20}H_{18}]^{2-}$, and $[ae\text{-}B_{20}H_{17}OH]^{4-}$.

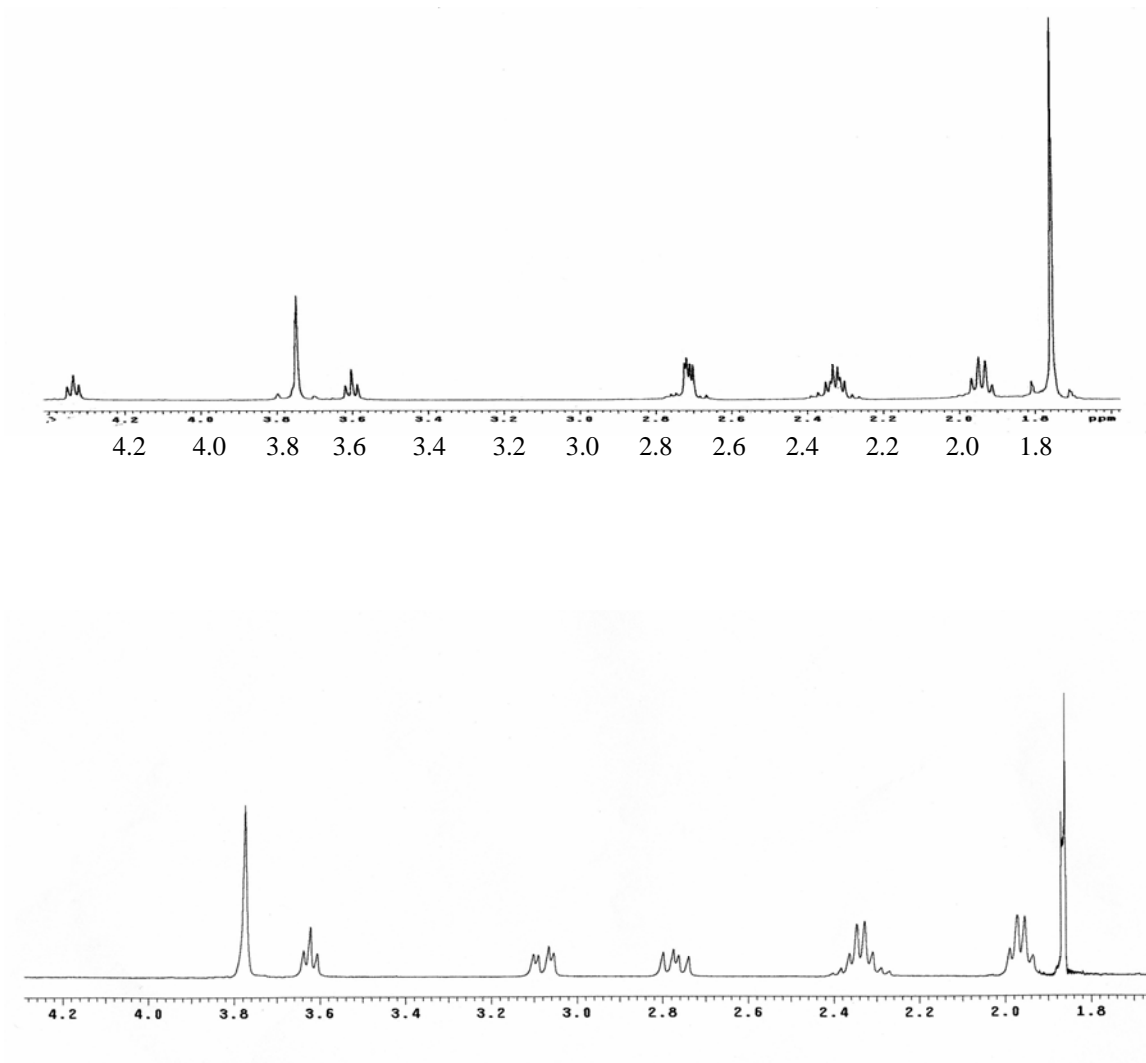|	Glutamyl			Cysteine		Glycine
	α	β	γ	α	β	γ
Reduced glutathione	54.7	26.2	29.1	55.7	25.3	42.1
Oxidized glutathione	53.1	26.5	31.2	54.3	39.1	42.1
Glutathione & $[a^2\text{-}B_{20}H_{17}SH]^{4-}$	53.1	26.3	29.6	54.4	39.1	43.5
Glutathione & $[n\text{-}B_{20}H_{18}]^{2-}$	54.1	26.2	29.7	55.8	25.4	42.1
Glutathione & $[ae\text{-}B_{20}H_{17}OH]^{4-}$	54.7	26.2	29.1	55.7	25.3	42.1

Figure 9: ^{1}H NMR spectrum of reduced glutathione (top) and ^{1}H NMR spectrum of oxidized glutathione (bottom).

carbon signals at 55.7 and 25.3 ppm, respectively. The α-carbon of the glycine residue, at 3.76 ppm, was correlated to the carbon signal at 29.1 ppm. These assignments are consistent with accepted literature values[28] and confirm the assignment for each of the atoms.

The COSY and HETCOR experiment confirm the assignments of the carbon atoms in reduced and oxidized glutathione. The carbon signal at 39.1 ppm in the oxidized glutathione is diagnostic for the formation of a disulfide bond. The signal at 39.1 ppm is attributed to the ß-carbon because of the cross-coupling of the proton signal at 3.64 ppm in the ^{1}H NMR spectrum of oxidized glutathione with the carbon signal at 39.1 ppm in the ^{13}C NMR spectrum (**Figure 14**). The assignments for the carbon signals at 55.7 ppm and 25.3 ppm were determined by COSY and HETCOR analysis. The peak at 55.7 ppm is assigned to the α-carbon of the cysteine residue and the peak at 25.3 ppm is assigned to the β-carbon of the cysteine residue. There is a clear shift, from 25.3 ppm to 39.1 ppm, for the β-carbon in the oxidized glutathione. A similar shift is also observed for the reaction of reduced glutathione and $K_4[a^2-B_{20}H_{17}SH]$. The lack of disappearance of the signal at 25 ppm, once again, indicates that the reaction was not complete. . The peak at 31.2 ppm is only observed in the oxidized glutathione and is assigned to the α-carbon of glycine. The carbon of the α-carbon in glycine shifted from 29.1 ppm to 31.2 ppm. The difference in signal is most like due to some rotation around the bond.[28]
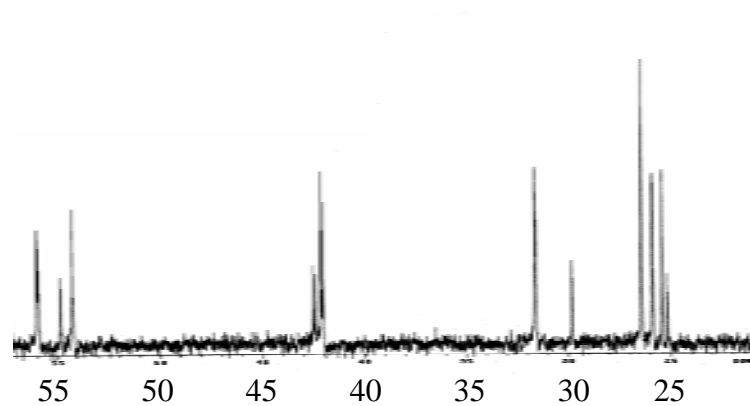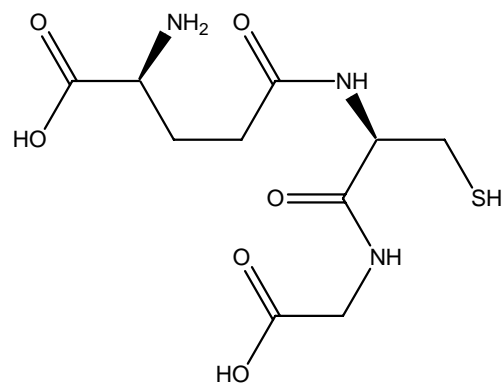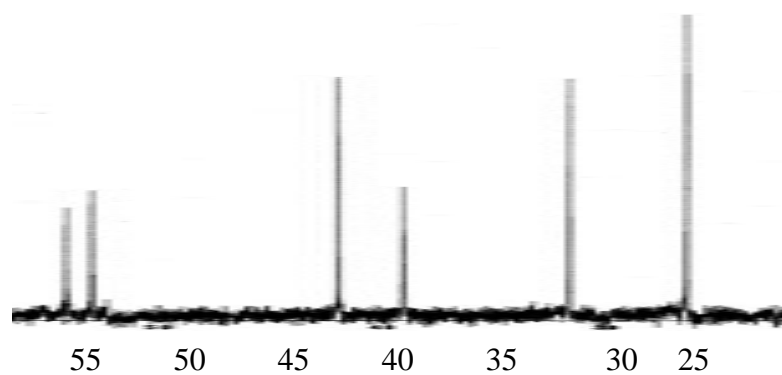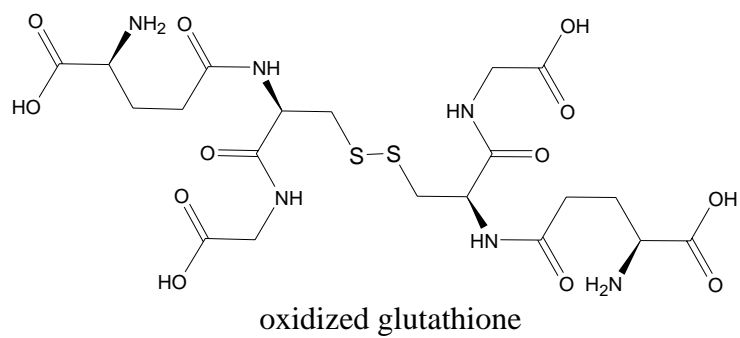
Figure 10: Comparison of the ^{13}C NMR spectra of oxidized glutathione (top), reduced glutathione (middle), and the reaction mixture of glutathione and the $[a^2\text{-}B_{20}H_{17}SH]^{4-}$ ion (bottom).

$[B_{20}H_{17}SH]^{4-}$ and reduced glutathione
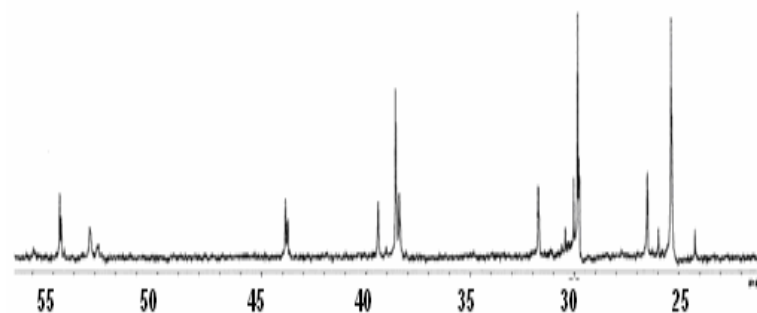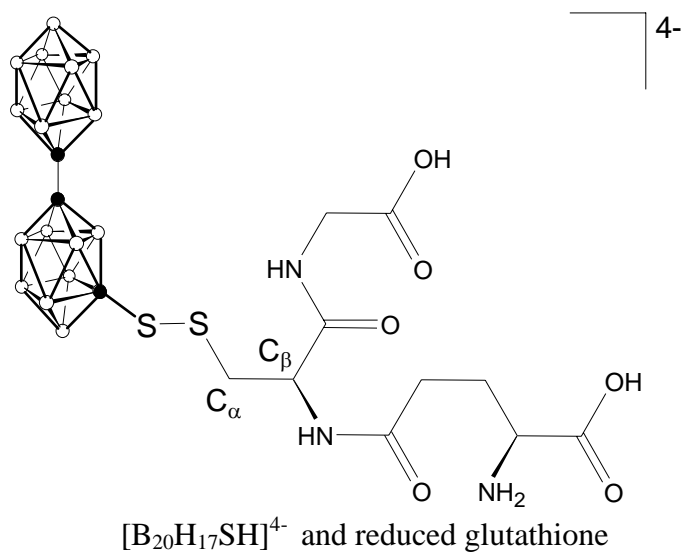
Figure 10 continued: Comparison of the ^{13}C NMR spectra of oxidized glutathione (top), reduced glutathione (middle), and the reaction mixture of glutathione and the $[a^2\text{-}B_{20}H_{17}SH]^{4-}$ ion (bottom).
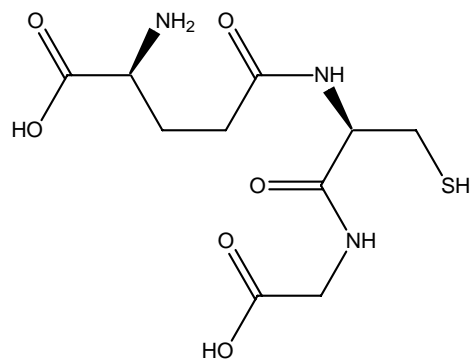
Reduced glutathione
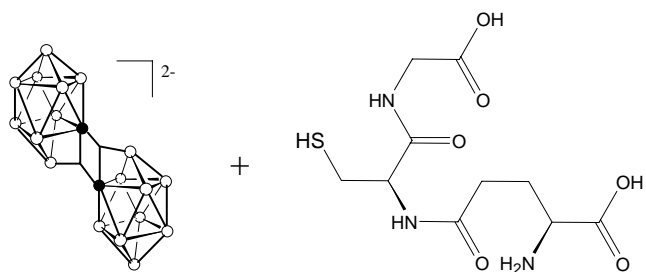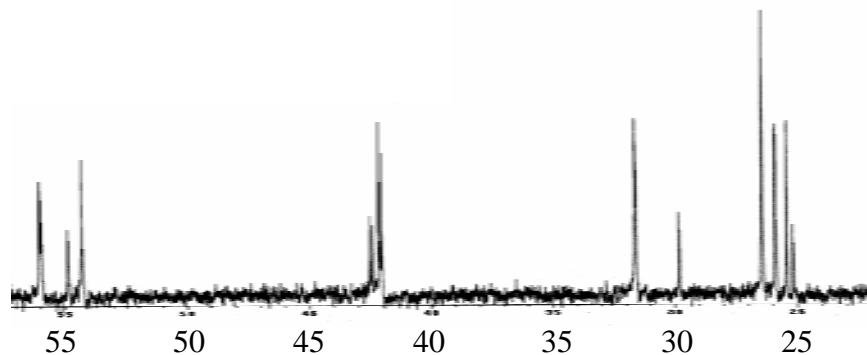
[n-B$_{20}$H$_{18}$] and reduced glutathione
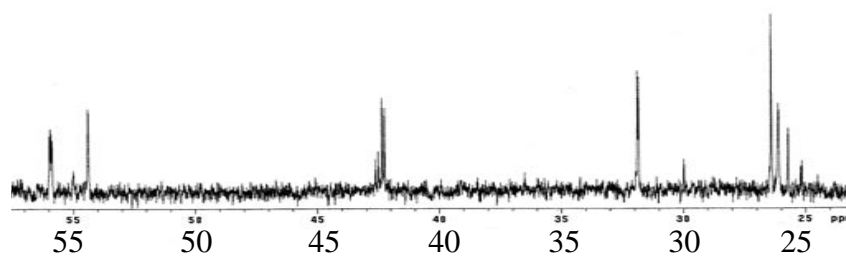
Figure 11: Comparison of ^{13}C NMR spectra of reduced glutathione (top), reaction mixture of the [n-B$_{20}$H$_{18}$]$^{2-}$ ion and reduced glutathione (middle), and reaction mixture of the [ae-B$_{20}$H$_{17}$OH]$^{4-}$ ion and reduced glutathione (bottom).

$[ae\text{-}B_{20}H_{17}OH]^{4-}$ and reduced glutathione
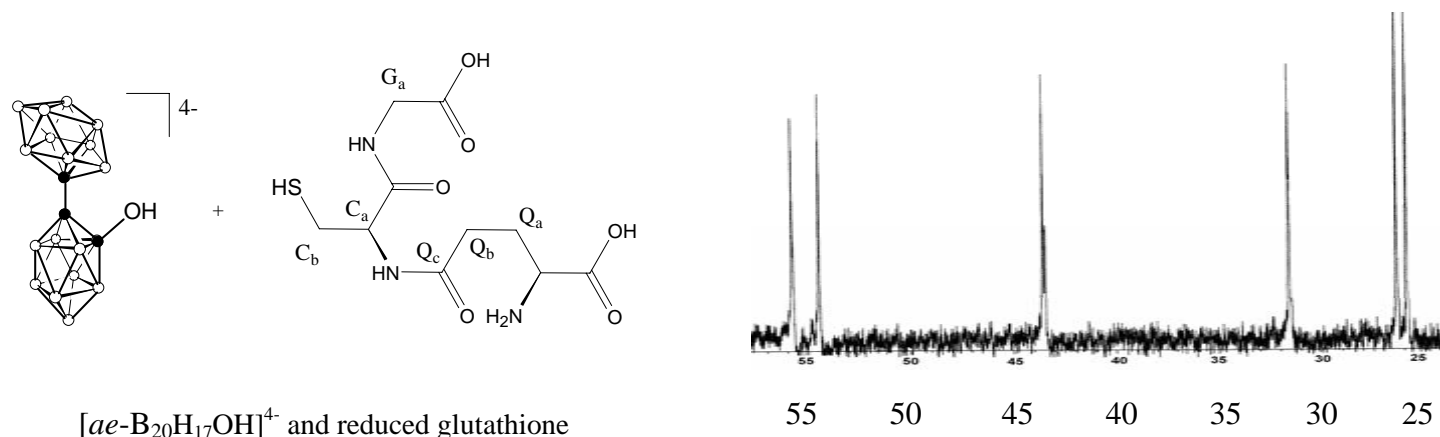
Figure 11 continued: Comparison of ^{13}C NMR spectra of reduced glutathione (top), reaction mixture of the $[n\text{-}B_{20}H_{18}]^{2-}$ ion and reduced glutathione (middle), and reaction mixture of the $[ae\text{-}B_{20}H_{17}OH]^{4-}$ ion and reduced glutathione (bottom).
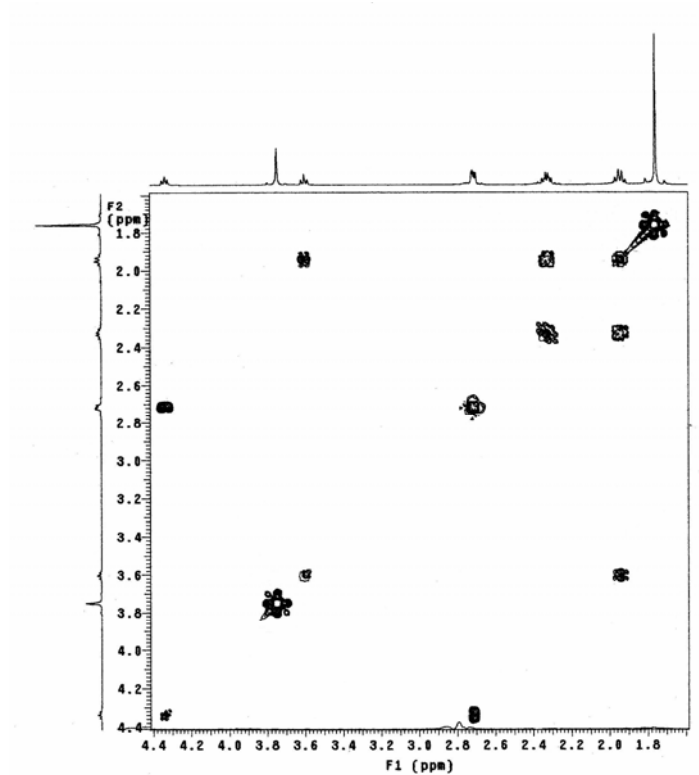
Figure 12: COSY of reduced glutathione.
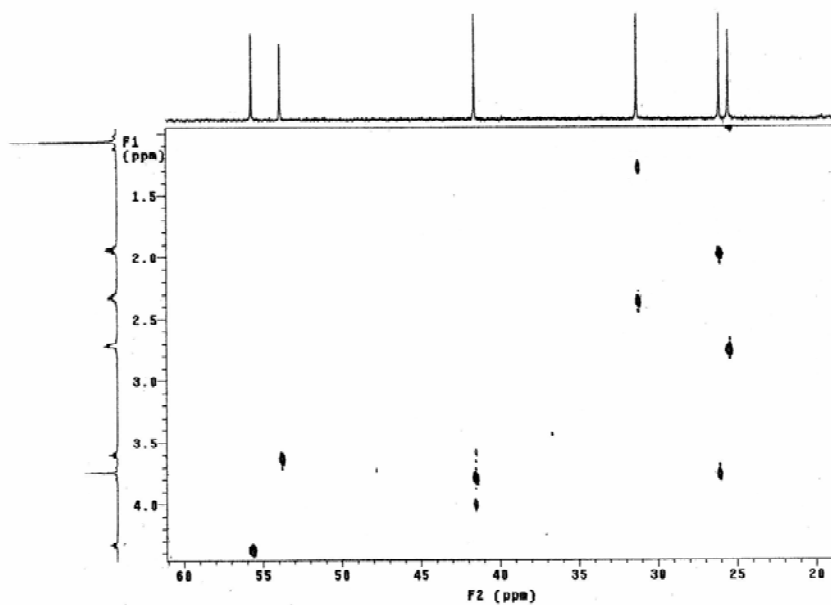
Figure 13: HETCOR of reduced glutathione.
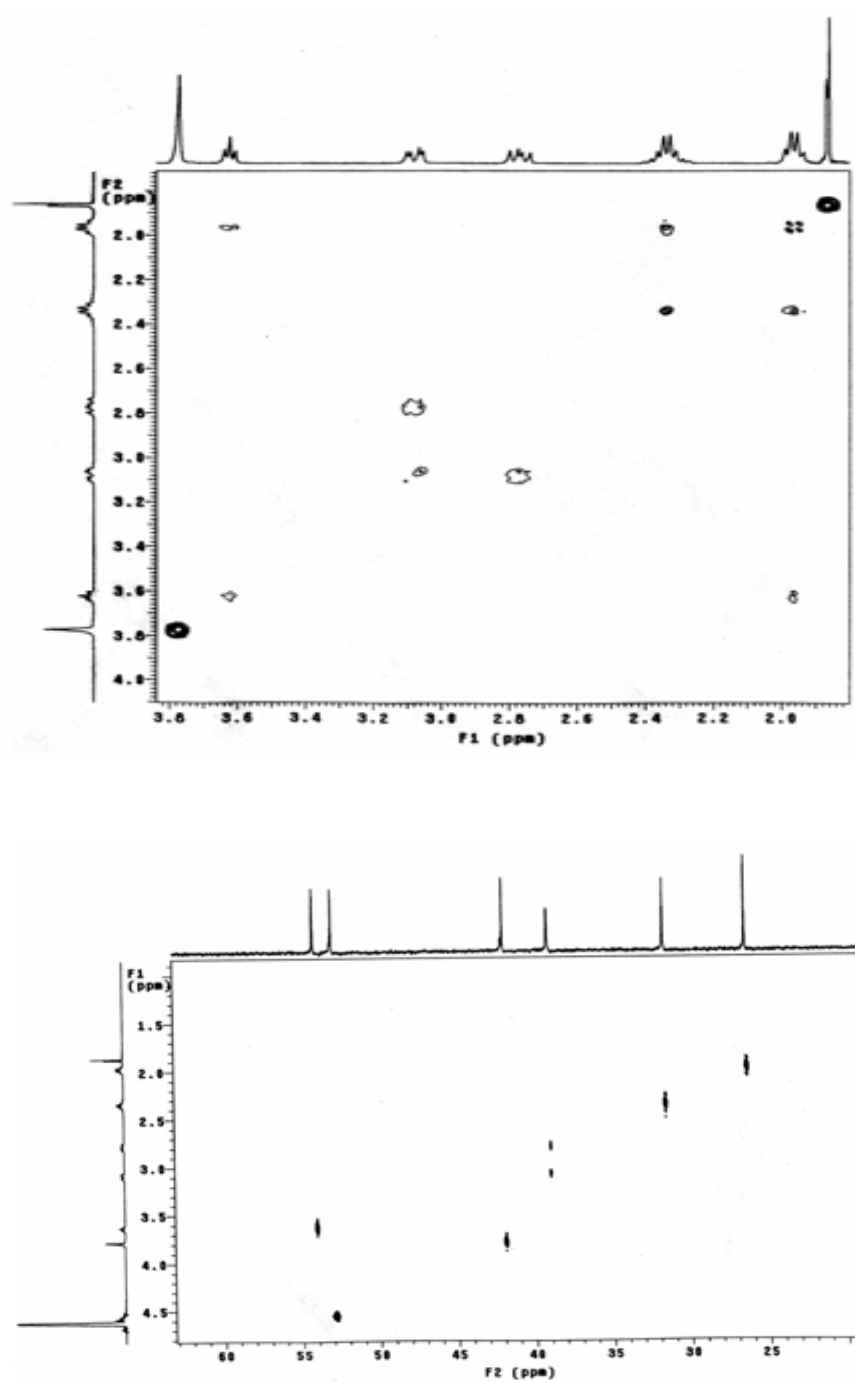
Figure 14: COSY (top) and HETCOR (bottom) of oxidized glutathione.

4.3 ESI Mass Spectrometry

Electrospray ionization (ESI) mass spectrometry creates ions by dispersing an analyte solution through a needle tip containing a high electrical field. The spray is heated and gas is applied to remove the solvent. The removal of the solvent increases the repulsion of charge above the surface tension and ions are ejected. ESI is the "softest" ionization method and is capable of detecting molecules that are bound through ionic interactions. In the current investigation, ESI was selected for its ability to analyze small molecules as a confirmation of the identity of the product. The ESI reports ions based on mass per unit charge (m/z) and like other spectrometry techniques, isotopes can be detected depending on there relative abundance. For atoms with sufficiently abundant isotopes and for compounds with a sufficient number of atoms, an isotopic envelope is created. The element boron has five isotopes. Two of the isotopes, the boron-10 and boron-11, are naturally occurring and three of the isotopes are artificial and short-lived, the boron-8, boron-12, and boron-13 isotopes.[29] The distribution of masses for the isotopes creates a unique boron envelope that will help characterized both the boron-containing starting compounds and the products of the reaction between the polyhedral borane anions and the selected biomolecules. The analysis of the ESI-MS data should enable the confirmation of the identity of the product and thus, the presence or absence of a new covalent bond in the reaction of the polyhedral borane anions and the reduced glutathione.

Evaluation of the Reduced Glutathione Reactions by ESI Mass Spectrometry. Previous examination of the reaction of reduced glutathione and the $[a^2\text{-}B_{20}H_{17}SH]^{4-}$ anion using NMR spectroscopy, indicated the formation of a covalent bond between the

$[a^2\text{-}B_{20}H_{17}SH]^{4-}$ anion and the sulfhydryl group of the cysteine amino acid. Reduced

glutathione will be used in the ESI experiments to confirm the identity of the product and

the formation of a new covalent bond. The low molecular weight of reduced glutathione

(307.3 g/m) and the polyhedral borane anions (218 g/mol to 266 g/mol) makes both the

starting materials and the reaction products well within the range of the ESI analysis. The

small molecular weight of the reaction products and the charged nature of the products

makes these reaction mixtures ideal for ESI-MS analysis.

Evaluation of the Reaction between Reduced Glutathione and Na₄[ae-B₂₀H₁₇OH]

by ESI Mass Spectrometry. Analysis of the pure $Na_4[ae\text{-}B_{20}H_{17}OH]$ starting material

produced a spectrum containing a boron-envelope with the central peak at 273.5 (**Figure

15**). This peak corresponds to the $[M+Na]^-$ and is the parent ion. Although the $Na_4[ae\text{-}$

$B_{20}H_{17}OH]$ species should have a 3- charge, it is not uncommon for the reduced

polyhedral borane anions to oxidize during the MS analysis. Therefore, the observed

species is actually $Na[B_{20}H_{17}OH]^-$. The predicted boron-envelope for the ion and the

actual boron-envelope in the ESI spectrum have extremely similar isotopic distribution.

The reaction of $Na_4[ae\text{-}B_{20}H_{17}OH]$ and reduced glutathione give the same parent ion

peak with no new additional peaks (**Figure 16**). Therefore there is no reaction between

the reduced glutathione and the $Na_4[ae\text{-}B_{20}H_{17}OH]$, consistent with the results obtained

from the NMR experiments.

Evaluation of the Reaction between Reduced Glutathione and Na₂[n-B₂₀H₁₈] by

ESI Mass Spectrometry. Analysis of the pure $Na_2[n\text{-}B_{20}H_{18}]$ starting material produced a

spectrum containing a boron envelope with the central peak at 257.4 (**Figure17**). This

peak corresponds to the $[M+K]^-$ and is the parent ion. Therefore, the observed species is

actually $K[n\text{-}B_{20}H_{18}]^-$. The presence of the potassium cation is from leaching of the glass

container while in storage. The predicted boron-envelope peak and the actual boron-

envelope in the ESI spectrum are well correlated. The ESI-MS spectrum of the reaction

of $Na_2[n\text{-}B_{20}H_{18}]$ and reduced glutathione yields the same parent ion peak with no new

additional peaks (**Figure 18**). Therefore, there is no reaction between the reduced

glutathione and the $Na_2[n\text{-}B_{20}H_{18}]$, consistent with the results obtained from the NMR

experiments. The absence of a new peak, which would correspond to the formation of the

product, provides sufficient evidence, that there is no reaction between the polyhedral

borane compounds, $Na_4[ae\text{-}B_{20}H_{17}OH]$ and $Na_2[n\text{-}B_{20}H_{18}]$, and the reduced glutathione.

   Evaluation of the Reaction between Reduced Glutathione and $K_4[a^2\text{-}B_{20}H_{17}SH]$ by

ESI Mass Spectrometry. Analysis of the pure $K_4[a^2\text{-}B_{20}H_{17}SH]$ starting material

produced a spectrum containing a boron-envelope with the central peak at 306.3 (**Figure**

19). This peak corresponds to the $[M+K]^-$ and is the parent ion. The predicted boron-

envelope and the actual envelope do not correlate as well as the previous compounds;

however, there appears to be overlapping signals at the m/z value. Although the $K_4[a^2\text{-}$

$B_{20}H_{17}SH]$ species should have a 3- charge, it is not uncommon for the reduced

polyhedral borane anions to oxidize during the MS analysis, as noted previously with the

$Na_4[ae\text{-}B_{20}H_{17}OH]$ compound.
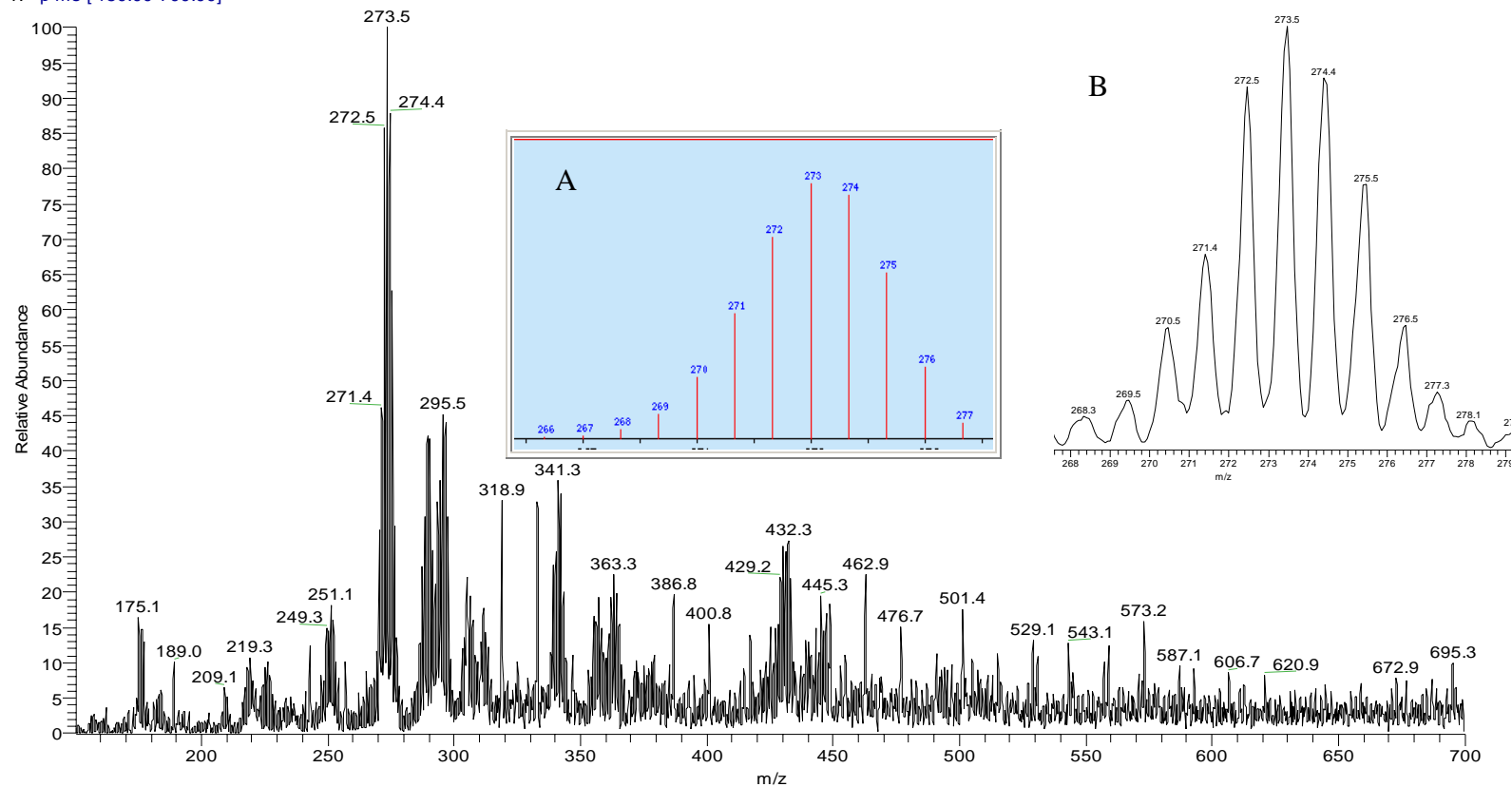
Figure 15: ESI-MS spectrum of unreacted Na$_4$[*ae*-B$_{20}$H$_{17}$OH]. Insets: A) the predicted spectrum of Na[*ae*-B$_{20}$H$_{17}$OH]$^-$ and B) expansion of the ion at 273 m/z in the actual spectrum.
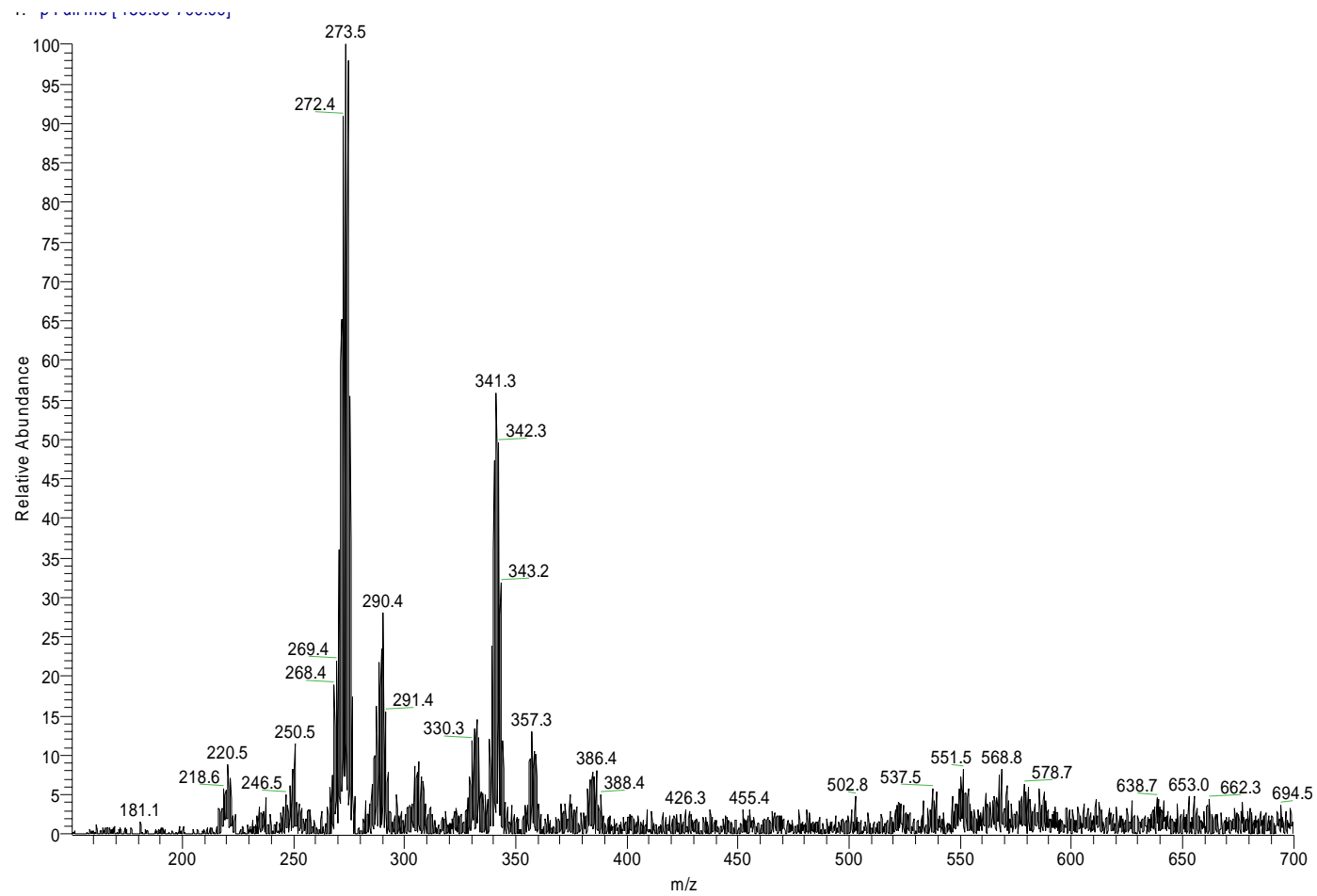
Figure 16: ESI-MS spectrum of the reaction of reduced glutathione and Na$_4$[*ae*-B$_{20}$H$_{17}$OH].
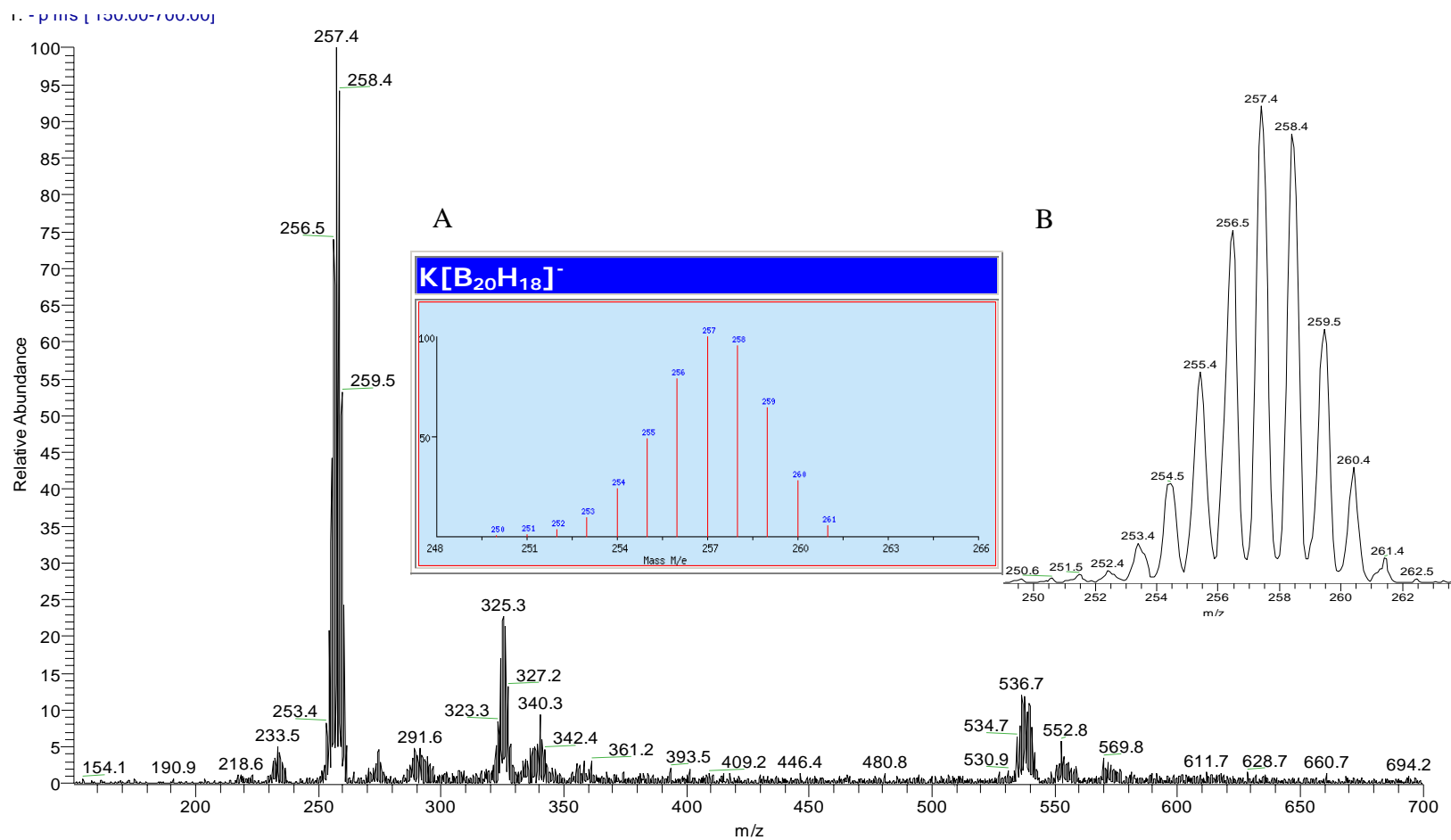
Figure 17: ESI-MS spectrum of unreacted $Na_2[n\text{-}B_{20}H_{18}]$. Insets: A) the predicted spectrum of $K[B_{20}H_{18}]^-$ and B) expansion of the ion at 257.4 m/z.
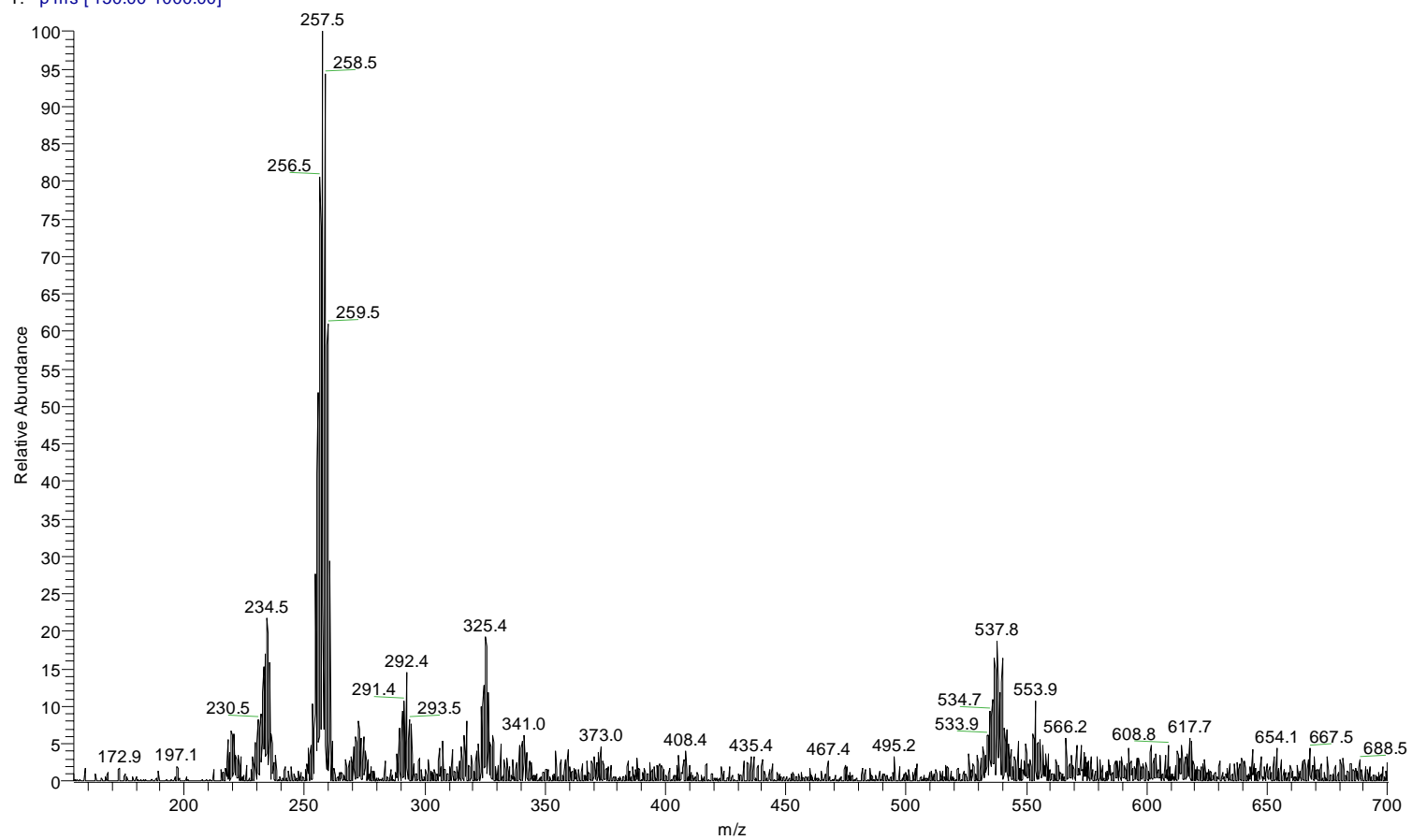
Figure 18: ESI-MS spectrum of the reaction of reduced glutathione and $Na_2[n\text{-}B_{20}H_{18}]$.
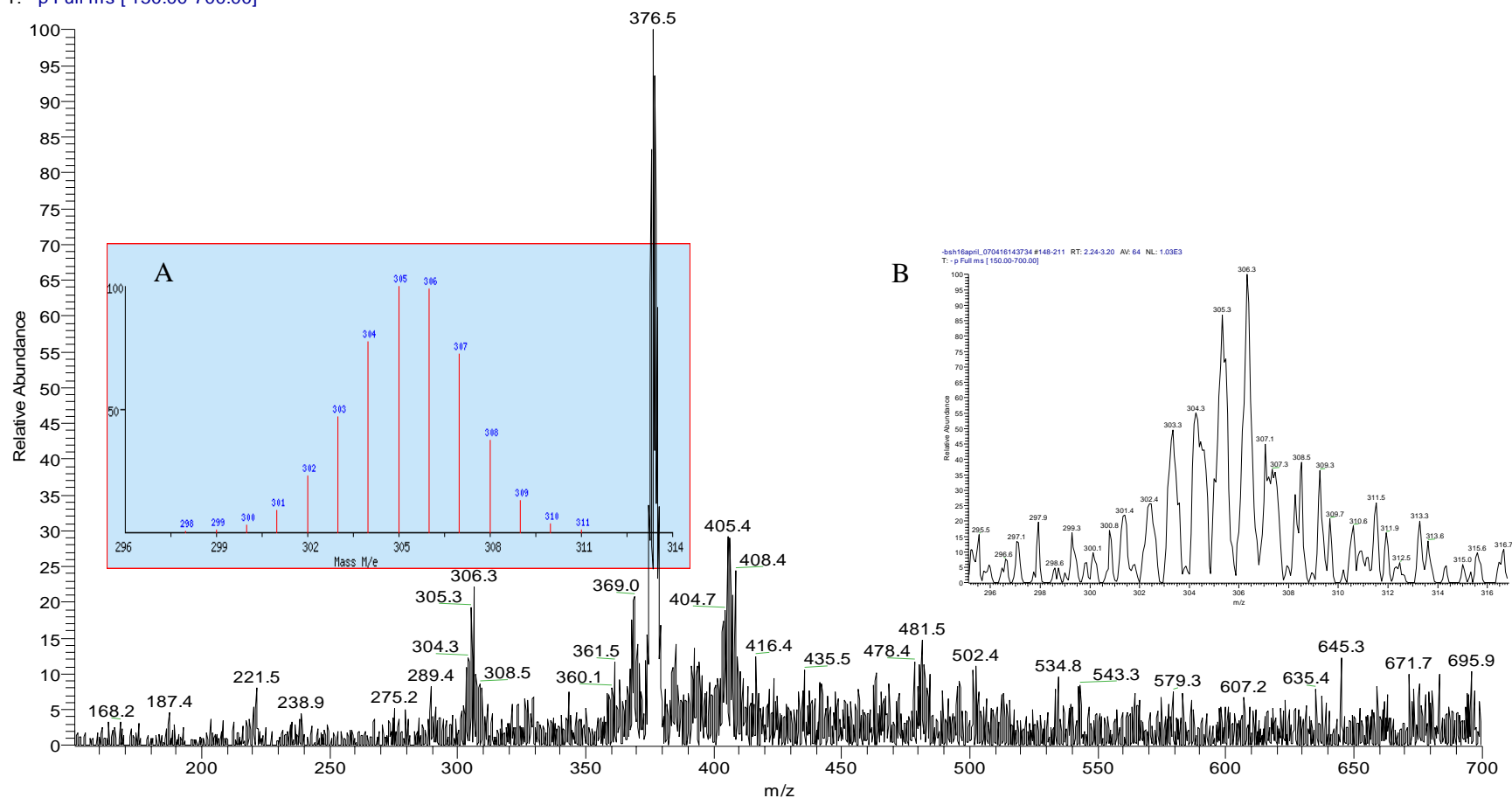
Figure 19: ESI-MS spectrum of unreacted $K_4[a^2$-$B_{20}H_{17}SH]$. Insets: A) the calculated spectra of $K[B_{20}H_{17}S]^-$ and B) expansion of the ion at 306.3 m/z.
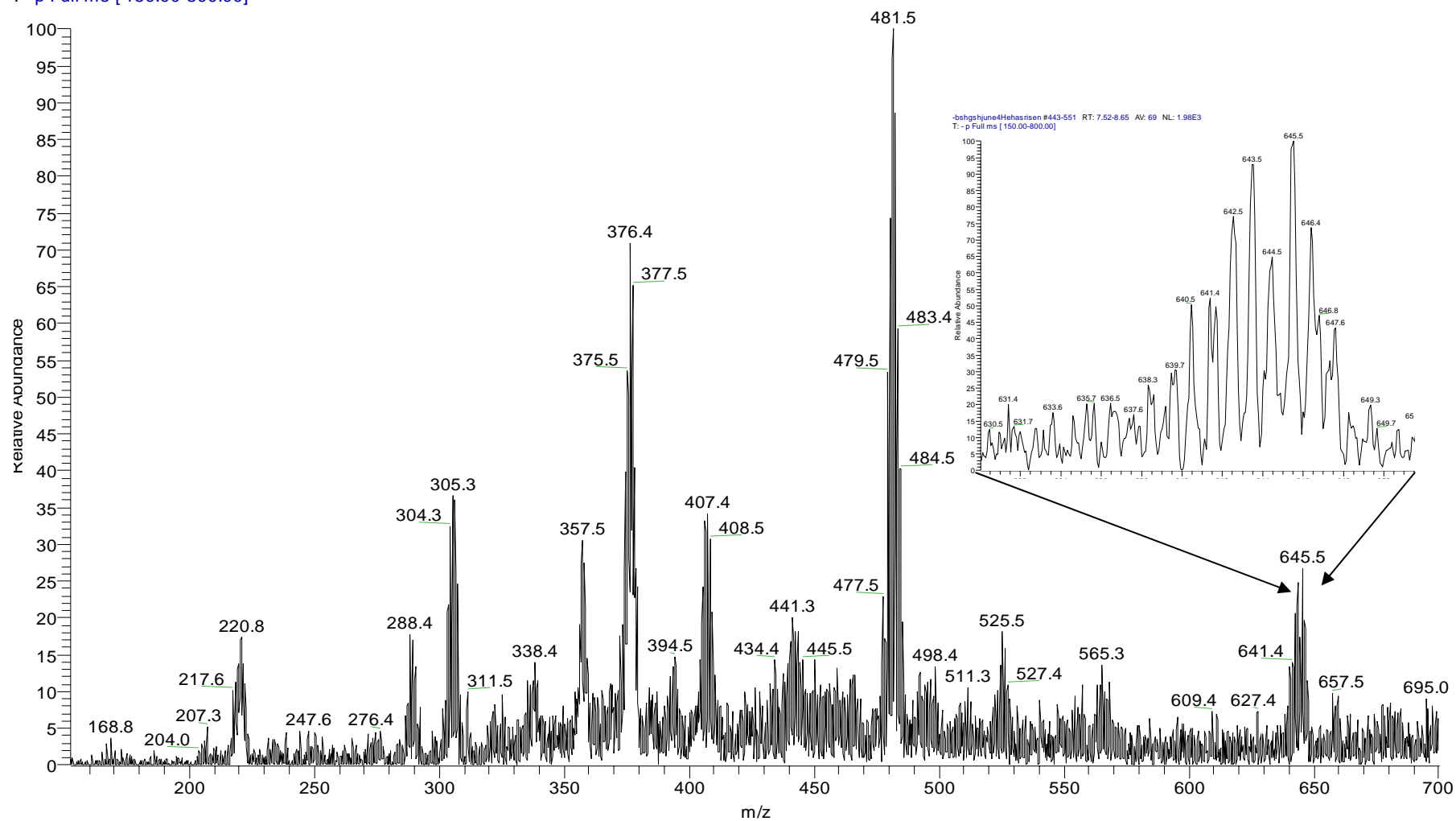
Figure 20: ESI-MS spectrum of the reaction of reduced glutathione and $K_4[a^2\text{-}B_{20}H_{17}SH]$. Inset: expansion of the ion at 645.5 m/z.

Therefore, the observed species is actually K[a^2-B$_{20}$H$_{17}$SH]$^-$. The spectrum of the

reaction mixture of K$_4$[a^2-B$_{20}$H$_{17}$SH] and reduced glutathione contains a peak at m/z

645.5 (**Figure 20**). The predicted peak of the formation a disulfide bond with out any

metal cations would be at 576.5 m/z. The ion at 645.5 m/z results from the formation of a

covalent bond between reduced glutathione and K$_4$[a^2-B$_{20}$H$_{17}$SH] and is consistent with

the results obtained from the NMR experiments. The interaction is a result of the free

sulfhydryl, since the other polyhedral borane anions, which did not have the sulfhydryl,

did not exhibit product formation with the reduced glutathione.

4.4 Gel Electrophoresis

Gel electrophoresis is used to separate high molecular weight compounds, such as

deoxyribonucleic acid (DNA) and proteins, based on various properties including: size,

charge, shape, isoelectric point, and affinity. The basic methodology is the use of a gel

matrix support in combination with an electromotive force that pulls or pushes the

molecule. In the case of protein electrophoresis, the gel is a cross-linked matrix formed

from polyacrylamide. The mixture is placed in a well and an electromotive force is

applied. The proteins are visualized using a protein stain.

Sodium dodecyl sulfate (SDS) is a surfactant which is added to most PAGE

experiments to disrupt the ionic interactions and also coat the proteins in a uniform

negative charge. The uniform negative charge causes the proteins to migrate through the

gel according to molecular weight. Native PAGE does not use SDS, heat denaturing, or

dithiothreitol (DTT) and is employed when undenatured proteins and, thus, the protein

disulfide bonds, are desirable**.** As a result, there is no uniform charge or shape, and the

proteins migrate according to charge, shape and size. While migration is difficult to predict, differences can be observed in the migration of a protein with or without a ligand.

Evaluation of HSA Reactions Using SDS-PAGE. Comparison of the control HSA, unreacted with the polyhedral borane ions, and the molecular weight standard, containing various known proteins and corresponding molecular weights, can be used to evaluate the size of the HSA protein. The difference in molecular weight of HSA and one of the polyhedral borane anions is a difference of hundreds, but the SDS-PAGE resolves differences in the thousands. The denaturing and reducing of the HSA before reaction with the $Na_4[a^2$-$B_{20}H_{17}SH]$ will result in the presence of 35 reduced, and potentially reactive, sulfhydryl residues. The increase in number of reactive sites should increase the number of $Na_4[a^2$-$B_{20}H_{17}SH]$ that can bind, resulting in a greater increase in molecular weight. The reactions will be treated with DTT which will reduce any disulfide formed between the HSA and $Na_4[a^2$-$B_{20}H_{17}SH]$. A change in the migration of the HSA and the polyhedral borane reaction mixtures not treated with DTT compared with the HSA and the polyhedral borane reaction mixtures treated with DTT would denote binding at the free sulfhydryls of the HSA. The increase should be significant and produce a noticeable change in migration, which has not been observed in previous SDS-PAGE experiments.

Lanes 4-7 of the first SDS-PAGE all contain a protein complex at the top of every lane (**Figure 21**). Lanes 2-5 in the first gel contain the reactions of stock HSA, unreacted HSA control, unfiltered DTT HAS and with $K_4[a^2$-$B_{20}H_{17}SH]$, and the filtered DTT HSA with $K_4[a^2$-$B_{20}H_{17}SH]$. The reactions in lanes 6-9 were not treated to DTT and contain
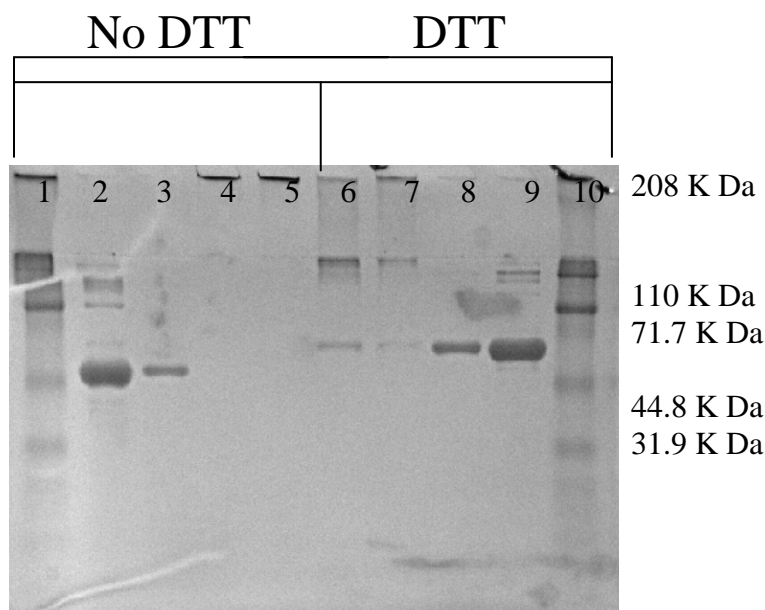
Figure 21: 10% Tris-Glycine SDS-PAGE of HSA. Lanes 1: the molecular weight ladder; Lane 2: stock HSA without DTT; Lane 3 unreacted HSA control without DTT; Lane 4: unfiltered HSA and $[a^2\text{-}B_{20}H_{17}SH]^{4-}$ without DTT; Lane 5: filtered HSA without DTT; Lane 6: filtered HSA and $[a^2\text{-}B_{20}H_{17}SH]^{4-}$, reduced with DTT; Lane 7: unfiltered HSA and $[a^2\text{-}B_{20}H_{17}SH]^{4-}$, reduced with DTT; Lane 8: unreacted HSA control, reduced with DTT; Lane 9: stock HSA, reduced with DTT; Lane 10: the molecular weight ladder.

the reactions of filtered denatured HSA, unfiltered denatured HAS, and the stock HSA with $Na_4[a^2\text{-}B_{20}H_{17}SH]$. The sample of stock HSA and control treated with DTT and both of the samples of each that were not treated do not contain the protein complex. The complex is unique to the reaction mixtures of undenatured HSA with $Na_4[a^2\text{-}B_{20}H_{17}SH]$. The protein complex is attributed to the denatured and reduced HSA reforming bonding with itself. The control HSA was denatured prior to the experiment and did not react under the same conditions as the polyhedral borane reactions, and as a result, a second SDS-PAGE experiment was performed

The second gel contains no protein complex for the unreduced frozen HSA sample and the unreacted HSA control in lanes 2 and 3 (**Figure 22**). The protein complex is present in the non-reduced HSA control in lane 4 but not in the reduced

frozen HSA in the protein complex in the unreacted denatured HSA control. The lack of appearance in the frozen denatured HSA demonstrates that the presence of the dark band in the reaction mixture of the HSA and $Na_4[a^2$-$B_{20}H_{17}SH]$ is not due to the $Na_4[a^2$-$B_{20}H_{17}SH]$ associating with the HSA, but the HSA bonding with itself.
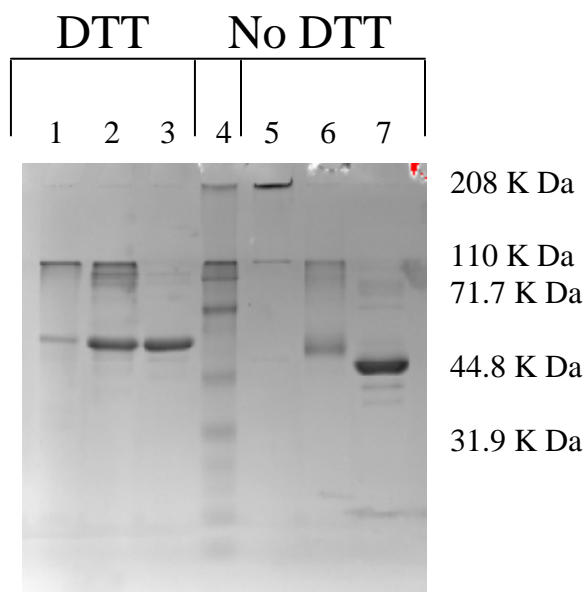
Figure 22: 10% Tris-Glycine SDS-PAGE of denatured HSA. Lane 1: denatured HSA reacted for 36 hr at 37 ° C reduced with DTT, Lane 2: denatured then frozen HSA, reduced with DTT; Lane 3: stock HSA, reduced with DTT; Lane 4: is the molecular weight ladder; Lane5: denatured HSA reacted for 36 hr at 37 ° C without DTT; Lane 6: denatured then frozen HSA without DTT; Lane 7: stock HSA without DTT.

Evaluation of HSA Reactions Using Native PAGE. The lack of SDS and reducing agents in the native PAGE will allow $Na_2[n$-$B_{20}H_{18}]$, $K_4[a^2$-$B_{20}H_{17}SH]$ and $Na_2[ae$-$B_{20}H_{17}OH]$ to interact with the HSA through either covalent or ionic bonds. Interactions will result in a difference in migration relative to the control HSA. If all three reaction mixtures exhibit a variation in migration, the interactions would most likely be attributed to the presence of strong ionic interactions, based on the MALDI-TOF experiments. In

contrast, if only one or two reactive polyhedral borane compounds, $Na_2[n\text{-}B_{20}H_{18}]$ and

$K_4[a^2\text{-}B_{20}H_{17}SH]$, exhibit variation in the migration, then covalent bonding is likely to be

present.

The native PAGE results are shown in **Figure 23**. The first, third, and fifth lanes

contain the HSA reacted with each anion: $[n\text{-}B_{20}H_{18}]^{2\text{-}}$, $[a^2\text{-}B_{20}H_{17}SH]^{4\text{-}}$, and $[ae\text{-}$

$B_{20}H_{17}OH]^{4\text{-}}$, respectively.
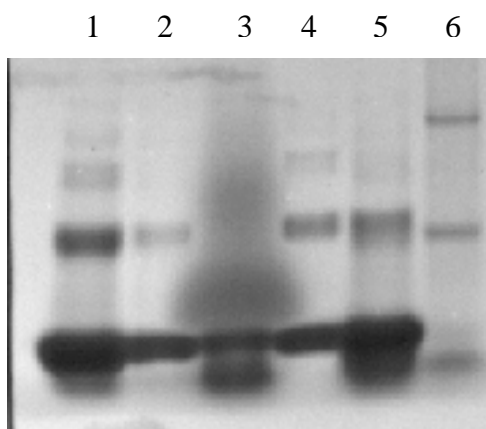
Figure 23: 10% Tris-Acetate Native PAGE of HSA. Lane 1: HSA and $Na_2[n\text{-}B_{20}H_{18}]$;
Lane 2: HSA control; Lane 3: HSA and $K_4[a^2\text{-}B_{20}H_{17}SH]$; Lane 4: the HSA control; Lane
5: HSA and $Na_4[ae\text{-}B_{20}H_{17}OH]$; Lane 6: the molecular weight ladder

The second and third lanes are the control HSA which was allowed to react under the

same conditions, but without any polyhedral borane anions present. The sixth and final

lane contains the molecular weight ladder. The control gels migrate in a similar manner

as reported in the literature.[29] The first lane of the gel, containing the product of the

reaction between HSA and $Na_2[n\text{-}B_{20}H_{18}]$, and the fifth lane, containing the product of

reaction between HSA and $Na_4[ae\text{-}B_{20}H_{17}OH]$, showed no difference with either HSA

control lanes. The significant change in migration is observed in the third lane which

contains the product formed from the reaction of HSA and $K_4[a^2\text{-}B_{20}H_{17}SH]$. The third

lane has a band in two places that do not exist in any of the other lanes. The unique migration patterns are most likely due to the formation of a covalent bond between $K_4[a^2\text{-}B_{20}H_{17}SH]$ and HSA.

4.5 MALDI-TOF Mass Spectrometry

The MALDI-TOF mass spectrometer ionizes samples that are dissolved in a matrix by glancing blasts from a laser. The blasts from the laser cause the matrix to volatilize and the sample is concurrently vaporized. The vapor travels down a time of flight (TOF) analyzer in which the sample are assigned m/z value bases on the time required to move down the apparatus to the analyzer. Larger ions migrate slower than smaller ions and are separated by m/z, making TOF advantageous for the analysis of protein digests. The MALDI-TOF mass spectra, in combination with trypsin digest, will be used to evaluate the presence of a covalent bond between the $[a^2\text{-}B_{20}H_{17}SH]^{4-}$ ion and the cysteine-34 residue of HSA. The results from the experiment should confirm the possible covalent binding of the HSA and the $[a^2\text{-}B_{20}H_{17}SH]^{4-}$ ion observed in the native PAGE of the current project and the DTNB experiments previously completed. [20]

Evaluation of the MALDI-MS Spectrum of the Control HSA. The digest of the control HSA should produce an ion at m/z 2459.9291,[31] which would correspond to the fragment containing the cysteine-34 residue of HSA. The covalent binding of the $[a^2\text{-}B_{20}H_{17}SH]^{4-}$ ion and the cysteine-34 should produce a mass m/z of 2725.929 in the spectrum of the product formed from the reaction of HSA and the $[a^2\text{-}B_{20}H_{17}SH]^{4-}$ ion.

Analysis of the control HSA digest produced a spectrum containing eight of the peaks predicted using standard software programs (**Table III**).

Table III: Mass from m/z 1213.3598 to 2053.45 of observed and predicted ions for MALDI analysis of trypsin digest of HSA.

Experimental Mass	Theoretical Mass	Modification	Residues	
1213.549	1213.3598		565	574
1215.565	1214.4627		437	445
	1227.3675		11	20
	1229.4961	pyroGlu	196	205
	1246.5267		196	205
1253.078	1253.4494		223	233
	1279.5758		429	439
	1297.5002		349	359
	1308.5762		535	545
	1312.5642		338	348
	1334.6061		277	286
	1343.5507		546	557
	1353.617		403	413
	1359.55	1Met-ox	546	557
	1400.5816		163	174
1412.783	1413.7329		175	186
	1425.5997		1	12
	1429.7136		433	444
	1451.7415		198	209
	1458.5965		263	274
	1463.657		82	93
	1468.7528		337	348
	1474.7977	pyroGlu	526	538
	1479.6564	1Met-ox	82	93
	1481.7922		403	414
	1481.8302	pyroGlu	522	534
	1491.8283		526	538
	1495.7706		473	484
	1498.8609		522	534
	1504.7891		210	222
	1509.7647		206	218
1511.851	1512.757		415	428
	1514.6174		561	573
	1519.6616		182	195
	1527.6355		52	64
	1530.8273		213	225
	1556.8381		200	212
	1575.9418		275	286
	1595.8261		360	372
1620.669	1620.0035		525	538
	1624.9106		324	336
	1624.9791		338	351
	1640.9099	1Met-ox	324	336
1639.89	1640.9322		414	428
	1642.7926		561	574
	1651.909		226	240
	1655.8347	pyroGlu	390	402
2053.84	2053.4245		414	432

Some of the peaks may have had their m/z altered as a result of not reducing the disulfide bonds. In that case, the ions would migrate as larger ions than the predictions. The presence of unreduced disulfide bonds do not, however, explain the absence of the target ion at m/z 2725.929 in the spectrum. The control digest spectrum contains intense keratin peaks due to contamination from skin during processing. The keratin peaks are observed in both spectra although the control digest spectrum does contain additional peaks which were not characterized (**Figure 24**).

The large amount of contamination from keratin results in a lower signal intensity for the desired HSA peaks and could cause some of the fragment masses to be missing in the control HSA digest. The validity of the control is lost due to the small number of fragments identified with the predicted mass and the target ion not being detected. Previous research using 25% ACN, as used in this project, resulted in an inability to detect the target ion at m/z 2459.9291, but when 50% ACN was used the target ion was detected.[31]
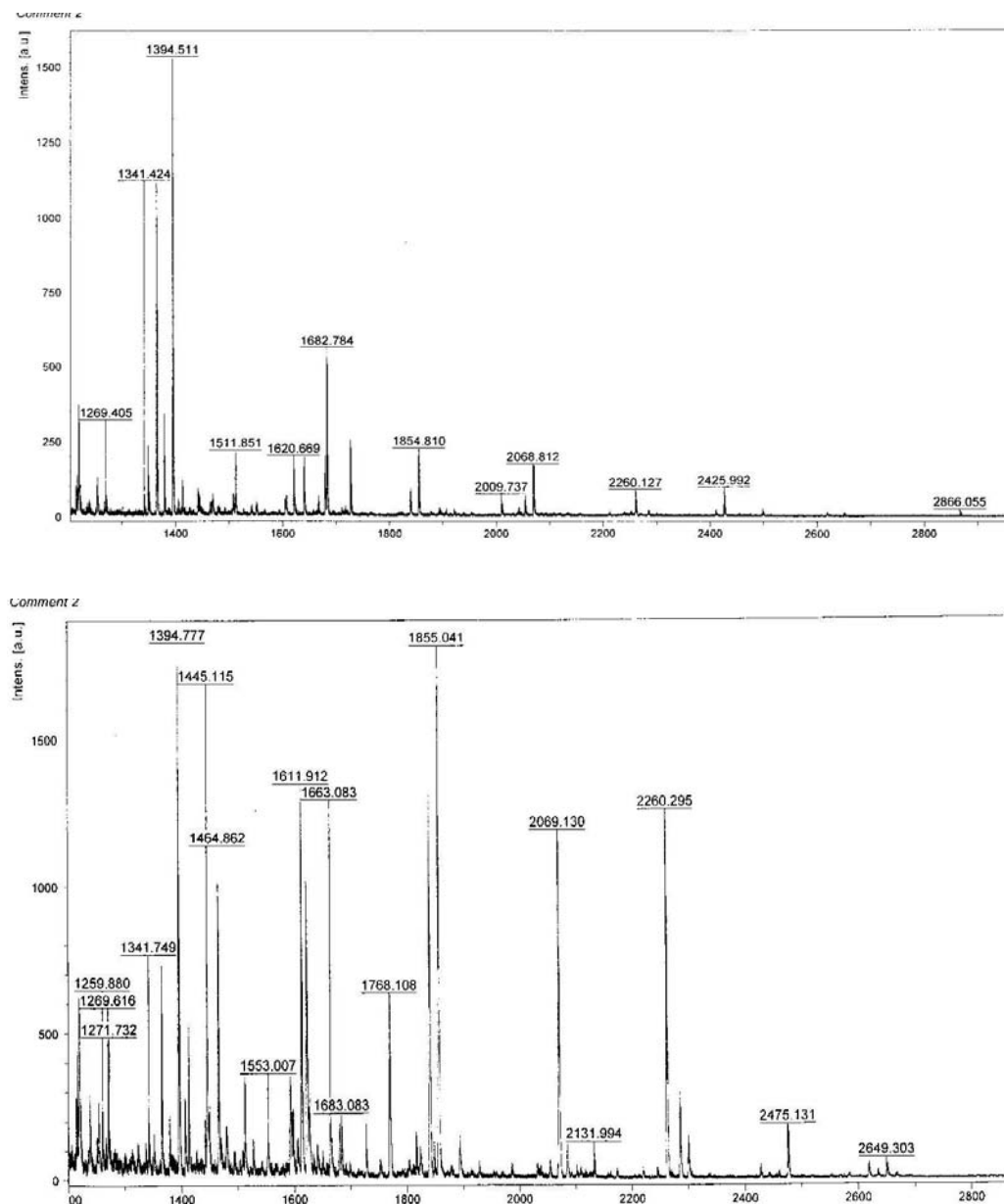
Figure 24: Comparison of the MALDI spectrum of the control HSA digest (top) with the MALDI spectrum of the trypsin digest of the reaction between HSA and the [a^2-B$_{20}$H$_{17}$SH]$^{4-}$ ion (bottom).

Evaluation of the MALDI-MS Spectrum of the Product Formed from the Reaction between HSA and K$_4$[a^2-B$_{20}$H$_{17}$SH]. The spectrum of the tryptic digest of the product formed from the reaction of HSA and K$_4$[a^2-B$_{20}$H$_{17}$SH] resulted in many of the same

peaks as the control HSA digest (**Figure 24**). There were unique peaks observed in the reaction spectrum, but they were not characterized. The detection of a difference in mass is not applicable since the target ion and few ions relating to the prediction for the control HSA were observed.

The MALDI-MS experiment could not produce the predicted values for the control HSA digest and, therefore, a basis for an increase in mass could not be established. Thus, an examination of the binding could not be obtained.

5.0 CONCLUSIONS

The goal of the research project was to determine the nature of the association, whether ionic or covalent, and the location of the association between a series of polyhedral borane ions and representative biomolecules. The polyhedral borane ions were selected based on their retention times in previously completed murine biodistribution experiments. Based on the results of previous biodistribution experiments, three mechanisms for the formation of covalent bonds between the polyhedral borane ions and intracellular protein moieties have been proposed: nucleophilic, oxidation followed by nucleophilic attack, and formation of disulfide bonds. The $[a^2\text{-}B_{20}H_{17}SH]^{4-}$ ion has the potential to react both by oxidation followed by nucleophilic attack and formation of disulfide bond. The ion, encapsulated in the unilamellar liposomes, exhibited an increase in tumor boron concentration over time in the murine trials. The $[n\text{-}B_{20}H_{18}]^{2-}$ ion can react only through nucleophilic attack and was retained in higher concentration in the tumor tissue when compared to the normal tissue. The $[ae\text{-}B_{20}H_{17}OH]^{4-}$ ion is known to be unreactive under physiological conditions and was cleared from both the tumor and normal tissue in the murine biodistribution trials. The polyhedral borane ions were allowed to react with cysteine, reduced glutathione and HSA at 37 ºC for 36 hr and then analyzed by ^{1}H and ^{13}C NMR spectroscopy experiments, SDS-PAGE, native PAGE, ESI-MS, and MALDI-TOF mass spectrometry. The results obtained for each ion will be summarized below.

The analysis of the product of the reaction between the $[a^2\text{-}B_{20}H_{17}SH]^{4-}$ ion and cysteine by ^{13}C NMR spectroscopy resulted in the appearance of two new carbon signals in the spectrum when compared with the spectrum of standard cysteine. The new peaks were similar in location to the carbon peaks of cystine, a disulfide-bonded homodimer of cysteine. The ^{13}C NMR spectrum of the reaction between reduced glutathione and the $[a^2\text{-}B_{20}H_{17}SH]^{4-}$ ion contains a new peak which is similar in location to the peaks assigned to the β-carbon of the cysteine residue in the ^{13}C NMR spectrum of oxidized glutathione. The assignment for the new peak was determined by COSY and HETCOR experiments. The ESI-MS of the product of the reaction between reduced glutathione and the $[a^2\text{-}B_{20}H_{17}SH]^{4-}$ ion resulted in the formation of a peak at 645.5 m/z, consistent with the formation of a disulfide bond. The lane of the native PAGE containing the product of the reaction between the HSA and the $[a^2\text{-}B_{20}H_{17}SH]^{4-}$ ion exhibited a difference in migration when compared with the control HSA. The native PAGE results are consistent with the formation of a strong bond between the $[a^2\text{-}B_{20}H_{17}SH]^{4-}$ ion and HSA. Therefore, the $[a^2\text{-}B_{20}H_{17}SH]^{4-}$ ion not only exhibited association with cysteine and reduced glutathione, but the association was confirmed at the sulfhydryl of cysteine. All results indicate the presence of a covalent bond between the polyhedral borane ion and the selected biomolecules.

The ^{13}C NMR spectrum of the product of the reaction between the $[n\text{-}B_{20}H_{18}]^{2-}$ ion and reduced glutathione contains no peaks that would be indicative of formation of the product resulting from nucleophilic attack. Likewise, the ESI-MS of the product of the reaction between the $[n\text{-}B_{20}H_{18}]^{2-}$ ion and reduced glutathione did not contain a peak consistent with product formation. The native PAGE gel of the reaction between HSA

and the $[n\text{-}B_{20}H_{18}]^{2-}$ ion produced no change in migration. The results from all the

experiments are consistent and conclude that a covalent bond was not found between the

$[n\text{-}B_{20}H_{18}]^{2-}$ ion and cysteine, reduced glutathione, or HSA, although there may be ionic

interaction present as suggested in previous research.[20]

The $[ae\text{-}B_{20}H_{17}OH]^{4-}$ ion is known to be unreactive at physiological conditions

and the results of this research were consistent with the known chemistry of the ion. The

^{13}C NMR spectra of the product of the reaction between the $[ae\text{-}B_{20}H_{17}OH]^{4-}$ ion and the

reduced glutathione contained no peaks that would be indicative of formation of any

product. The ESI-MS of the reaction mixture that contained reduced glutathione and the

$[ae\text{-}B_{20}H_{17}OH]^{4-}$ ion exhibited no new peaks when compared with ESI-MS of the

standard $[ae\text{-}B_{20}H_{17}OH]^{4-}$ ion and there was no change in migration in the native PAGE

of the HSA and the $[ae\text{-}B_{20}H_{17}OH]^{4}$ ion when compared with the HSA control.

Therefore, the $ae\text{-}B_{20}H_{17}OH]^{4-}$ ion does not form any strong association with the selected

biomolecules.

In summary, the $[a^2\text{-}B_{20}H_{17}SH]^{4-}$ ion was the only polyhedral borane anion

investigated to produce results consistent with formation of a covalent bond to the

selected biomolecules, cysteine, reduced glutathione, and HSA. In the case of the

cysteine and the reduced glutathione, a disulfide bond is formed at the free thiol of the

cysteine. The proposed covalent interactions with HSA is at the free thiol on the cysteine

34 residue. Although the $[n\text{-}B_{20}H_{18}]^{2-}$ and $[ae\text{-}B_{20}H_{17}OH]^{4-}$ ions exhibited no evidence of

covalent bond formation, the ions may associate to intracellular protein by electrostatic

interactions, as noted in earlier investigations.

Even though the MALDI-MS experiment will be repeated to receive the results that better match previous experiments,[20] the results obtained from the reduced glutathione experiments are particularly relevant to application of the polyhedral borane compounds in BNCT. An increase in cellular reduced glutathione levels has been associated with drug resistant cancer cells[27] and with less aggressive and earlier stage breast cancer, such as mammary adenocarcinoma.[32] Other projects have analyzed the use of buthionine sulphoximine (BSO) to inhibit reduced glutathione formation which reduced tumor cell proliferation.[33] While the HSA is inexpensive and well characterized, glutathione is far more involved in tumor cell growth and should be used as a standard for future experiments.

6.0 SUGGESTIONS FOR FUTURE RESEARCH

Although this research concluded, based on the NMR spectroscopy and ESI mass spectrometry, that a covalent bond was formed between the sulfhydryl in both the cysteine and the reduced glutathione and the sulfhydryl group of the $[a^2\text{-}B_{20}H_{17}SH]^{4-}$ ion, the evaluation of the products using supplementary techniques could provide additional support. For example, a Raman spectrum of the product containing the disulfide bond should have a different adsorption than the Raman spectrum of the starting material, which contains the free sulfhydryl substituent. Additionally, isolation of the individual products would enable an elemental analysis of the isolated compounds and identify the products unambiguously.

The mechanism of nucleophilic attack could be explored in greater detail by synthesizing specific peptides with amino acids containing highly nucleophilic groups. The peptides should be allowed to react with the same polyhedral borane ions, particularly the $[n\text{-}B_{20}H_{18}]^{2-}$ ion, and analyzed using the same methods as the current research project.

The MALDI-MS experiment should be repeated using more caution regarding potential contamination and also by altering some of the procedures. The contamination could be addressed by using hoods during all reaction sequences and by autoclaving and properly sterilizing all equipment. The change in procedure would be to use an aqueous

50% acetonitrile solution instead of an aqueous 20% acetonitrile solution, which was reported in the previous literature. The use of an aqueous 50% acetonitrile solution was the only solvent combination in the published paper that produced the target ion with the cysteine-34 in the spectrum.[31]

The results from these experiments would enable a more efficient and effective evaluation of the boron-containing compounds. The research would provide a better understanding of the potential mechanism(s) of retention for the polyhedral borane ions, once delivered by unilamellar liposomes. Characterization of the mechanism of the retention should assist in the design of future compounds with a high probability of success and potential application to BNCT, whose future depends on the development of the boron-containing compounds that can be delivered and retained in high concentrations in the tumor cells.

REFERENCES

1. Soloway, A. H., Tjarks, W., Barnum, B. A., Rong, R-G., Barth, R. F., Codogni, I. M. & Wilson, J. G. (1998) *Chem. Rev.* **98**, 1515-1562.

2. Salcman, M. *In Brain Tumors: An Encyclopedic Approach*; A. H. Laws, E. R., Jr., Eds; Churchill Livingstone; Edinburgh, 1995; p369.

3. Sano, K. *Neurosurg. Rev.* 1986**, 9**, 13.

4. Kornblith, P. L. & Walker, M. L. *Neurosurg.* 1988, **66**, 591-599.

5. Locher, G.L. (1936) *Am. J. Roentgenol. Radium Ther.* **36**, 1-13.

6. Fairchild, R. G. & Bond, V. P. (1985) *J. Radiat. Oncol. Biol. Phys.* **11**, 831-840.

7. Zhou, J., Soloway, A.H., Barnum, B.A., & Tjarks, W. *Frontiers in Neutron capture therapy* [Proceedings of the International Symposium of Neutron Capture Therapy for Cancer]. 8th, Los Angeles, CA, USA, Sept 13-18, 1998.

8. Gaun, L., Wims, L. A., Kane, R. R., Smuckler, M. B., Morrison, S. L. & Hawthorne, F. (1998) *Proc. Natl. Acad. Sci.* USA **95**, 1320-13210.

9. Shelly, K., Feakes, D. A., Hawthorne, M. F., Schmidt, P. G., Krisch, T. A. & Bauer, W. F. (1992) *Proc. Natl. Acad. Sci. USA* **89**, 9039-9043.

10. Radel, P. A. & Kahl, S. B. (1996) *J. Org. Chem.* **61**, 4582.

11. Srivastava, R. R. & Kabalka, G. W. (1997) *J. Org. Chem.* **62**, 8730-8734.

12. Srivastava, R. R., Singhaus, R. R. & Kabalka, G. W. (1997) *J. Org. Chem.* **62**, 4476-4478.

13. Feakes, D. A., Shelly, K., Knobler, C. B. & Hawthorne, M. F. (1994*) Proc. Natl. Acad. Sci. USA* **91**, 3029-3033.

14. Feakes, D.A., Shelly, K. & Hawthorne, M. F. (1995) *Proc. Natl. Acad. Sci USA* **92**, 1367-1370.

15. Feakes, D. A., Waller, R. C., Hathaway, D. K. & Morton, V. S. (1999) *Proc. Natl. Acad. Sci. USA* **96**, 6406-6410.

16. Straubinger, R. M., Hong, K., Friend, D. S. & Papahadjopoulos, D. (1983) *Cell* **32**, 1069-1079.

17. Georgiev, E. M., Shelly, K., Feakes, D. A., Kuniyoshi, J., Romano, S. & Hawthorne, M. F. (1996) *Inorg. Chem.* **35**, 5412-5416.

18. Tang, P. Z., Schweizer, M. P., Bauer, W. F., & Bradshaw, K. M. *Advances in Neutron Capture Therapy* [Proceedings of the International Symposium of Neutron Capture Therapy for Cancer]. 5th, Columbus Oh, USA, Sept 14-17, 1992.

19. Waller, R. C., Spinler, J. & Feakes, D. F. *Frontiers in Neutron Capture Therapy*, [Proceedings of the International Symposium of Neutron Capture Therapy for Cancer]. 5th, Columbus Oh, USA, Sept 13-18, 1998.

20. McVey, W. J. (2003) Masters of Science Thesis, Southwest Texas State University.

21. Kosower N. S. & Kosower E. M. (1978) *Int. Rev. Cytol.* **54**,109-160.

22. Feakes, D. A., Waller, R. C., Hathaway, D. K. & Morton, V. S. (1999) *Proc. Natl. Acad. Sci. USA* **96**, 6406-6410.

23. Hawthorne, M. F., Pilling, R. L. & Garrett, P. M. (1965) *J. Am. Chem. Soc.* **87**, 4740-4746.

24.   Hawthorne, M. F. & Pilling, R. L. (1967) *Inorg. Synth.* **9**, 16-19.

25.   Chamberland, B. L. & Muetterties, E. L. (1964) *Inorg. Chem.* **3**, 1450-1456.

26.   Daly, W. H. & Lee, C. S. (1973) *Polymer Preprints* **14**, 1238-1243.

27.   Meister, A. (1989) *Proc. Fed. Asiatic Oceanian Biochem. Congr.* 5th, 417-427.

28.   York, M. J., Beilharz, G. R. & Kuchel, P. W. (1987) *Int. J. Peptide Protein Res.* **29**, 638-646.

29.   Windhulz, M., Budavari, S., Blumetti, R. F., & Otterbein, E. S. (1983) *Mercks Index* 10th edition, 186.

30.   Lin, J., Meyer, J. D., Carpenter, J. F. & Manning, M. C. (2000) *Phamaceutical Research* **17**, 391-396.

31.   Wa, C., Cerny, R. & Hage, D. S. (2005) *Analytical Biochemistry* **349**, 229-241.

32.   Terradez, P., Asensi, M., Lasso de La Vega, M. C., Puertes, I. R., Vina, J. & Estrela, J. M. (1993) *Biochem. J.* **292**, 477-483.

VITA

Barrett Matthews was born in Houston, Texas, on September 3, 1976, the son of Peter J. Matthews and Tina A. Matthews. After completing high school at Brazoswood High School (Clute, Texas) in 1995, he entered Brazosport Community College. He worked off and on for seven years as a land surveyor to support himself through college. He graduated with a Bachelor of Science in Biochemistry from Texas State University-San Marcos in 2004.

Permanent Address: 250 Schely

                       Richwood, TX 77531

This thesis was typed by Barrett Matthews.